induced liver injury, it was reported that ICAM-1 expression and the resultant leukocyte infiltration are involved in the deterioration of alcohol-induced liver injury.[9] Therefore, the suppression of inflammatory responses may be achieved by selective knockdown of ICAM-1 in HECs.

RNA interference is an important endogenous mechanism for gene regulation by cleaving specific messenger RNA (mRNA) possessing the complementary sequence using small interfering RNA (siRNA).[10,11] Although siRNA is a promising candidate for molecular therapy, an effective method for siRNA transfer into the cytoplasm of targeted cells *in vivo* is still being developed. The effective methods for *in vivo* siRNA delivery involve nonviral carriers, including liposomes, emulsions, micelles, and polymers.[12-18] However, because the nonviral carriers are taken up into the cells via endocytosis, degradation within endosomes and escape from endosomes are major obstacles for the improvement of siRNA therapeutics. Moreover, efficient and selective siRNA delivery into HECs is essential to achieve the potent anti-inflammatory effects produced by ICAM-1 siRNA.

Recently, the benefits have become appreciated of delivery of nucleic acids into cells using microbubbles and ultrasound (US) (also known as "sonoporation methods"), due to the high transfer efficiency into the cytoplasm.[19-22] Our group has developed US-responsive and mannose-modified liposomes/plasmid DNA complexes for *in vivo* gene transfer and successfully obtained efficient gene expression in mannose receptor-expressing cells, such as HECs and splenic dendritic cells.[23-25] Moreover, we demonstrated that a large amount of plasmid DNA could be directly transferred into the cytoplasm through a mechanism involving transient pores created on the cell membrane by the destruction of microbubbles after US exposure.[26] Therefore, the efficient transfer of ICAM-1 siRNA into HECs might be achieved by applying this method to siRNA delivery.

In the present study, we developed an ICAM-1 siRNA transfer system based on US-responsive and mannose-modified liposome/siRNA complexes (Man-PEG_{2000} bubble lipoplexes [Man-PEG_{2000} BLs]) for anti-inflammatory therapy. ICAM-1 siRNA delivered by Man-PEG_{2000} BLs and US exposure was selectively and efficiently transferred into HECs *in vitro* and *in vivo*. Furthermore, sufficient ICAM-1 suppression and potent anti-inflammatory effects were achieved by ICAM-1 siRNA transfer against various types of inflammation induced by lipopolysaccharide (LPS), dimethylnitrosamine (DMN), carbon tetrachloride (CCl_4), and IR. To our knowledge, this is the first report of a gene transfer method using Man-PEG_{2000} BLs and US exposure for the selective and efficient transfer of siRNA to HECs. This novel siRNA transfer method could be valuable for medical treatments that target HECs.

Materials and Methods

In vitro *siRNA Delivery*. After incubation of HECs for 72 hours, the culture medium was replaced with Opti-MEM I (Invitrogen, Carlsbad, CA) containing lipoplexes/BLs (1 μg siRNA). At 5 minutes after siRNA transfer, HECs were exposed to US (frequency, 2.062 MHz; duty, 50%; burst rate, 10 Hz; intensity, 4.0 W/cm^2) for 20 seconds. In the siRNA delivery using naked siRNA and conventional nanobubbles, at 5 minutes after addition of naked siRNA (1 μg) and conventional nanobubbles (60 μg total lipids), cells were immediately exposed to US. US was generated using a Sonopore-4000 sonicator (Nepa Gene, Chiba, Japan). At 1 hour after US exposure, the medium was replaced with RPMI-1640 and incubated for an additional 23 hours. Lipofectamine 2000 (Invitrogen) was used according to the recommended procedures with an exposure time of 1 hour, which is the same exposure time in other experiments using lipoplexes.

In Vivo *siRNA Delivery*. Six-week-old C57BL/6 female mice were intravenously injected with BLs containing 10 μg siRNA via the tail vein. At 5 minutes after the injection of the bubble lipoplexes, US (frequency, 1.045 MHz; duty, 50%; burst rate, 10 Hz; intensity 1.0 W/cm^2; time, 2 minutes) was applied transdermally to the abdominal area using a Sonopore-4000 sonicator. In the siRNA delivery using naked siRNA and conventional nanobubbles, at 4 minutes after intravenous injection of conventional nanobubbles (500 μg total lipid), naked siRNA (10 μg) was intravenously injected and US was exposed at 1 minute after naked siRNA injection.

Address reprint requests to: Mitsuru Hashida, Ph.D., and Shigeru Kawakami, Ph.D, Department of Drug Delivery Research, Graduate School of Pharmaceutical Sciences, Kyoto University, 46-29 Yoshida-shimoadachi-cho, Sakyo-ku, Kyoto 606-8501, Japan. E-mail: hashidam@pharm.kyoto-u.ac.jp (Mitsuru Hashida) and kawakami@pharm.kyoto-u.ac.jp (Shigeru Kawakami); fax: (81)-75-753-4575.

View this article online at wileyonlinelibrary.com.

DOI 10.1002/hep.25607

Potential conflict of interest: Nothing to report.

Additional Supporting Information may be found in the online version of this article.

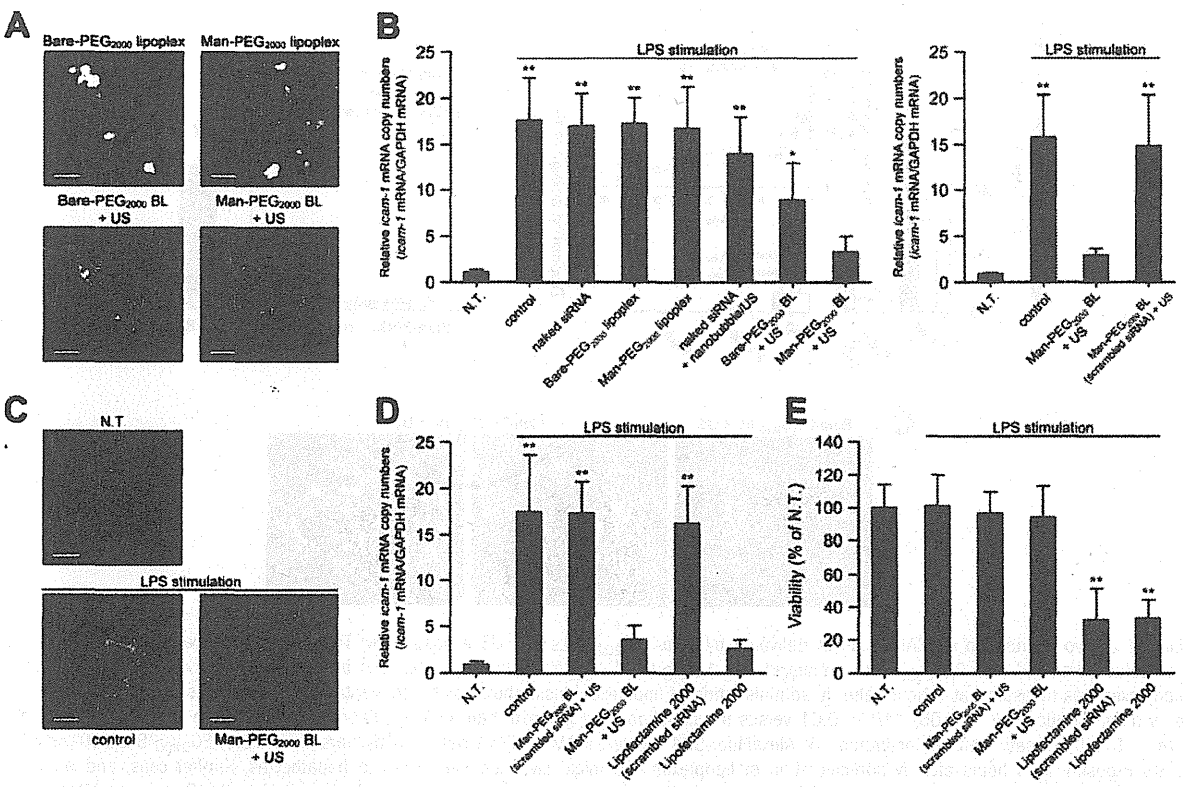

Fig. 1. Suppression effects of *icam-1* mRNA expression and cytotoxicity followed by ICAM-1 siRNA delivery in LPS-stimulated primary mouse HECs. (A) *In vitro* confocal images of cellular associated ICAM-1 siRNA (1 μg siRNA) transferred by various methods 1 hour after treatment in primary mouse HECs. US was directly exposed to HECs at 5 minutes after addition of BLs. The lipoplexes were constructed with AlexaFluor-594-labeled ICAM-1 siRNA (red), and the endosomes were labeled with AlexaFluor-488 transferrin conjugates (green). Nuclei were counterstained with 4′,6-diamidino-2-phenylindole (DAPI) (blue). Scale bars, 10 μm. (B,C) The level of *icam-1* mRNA expression (B) and *in vitro* confocal images of ICAM-1 expression (C) obtained by ICAM-1 siRNA transfer (1 μg siRNA) using various types of methods 24 hours after LPS stimulation in primary mouse HECs. US was directly exposed to HECs at 5 minutes after addition of BLs, and cells were exposed to LPS (100 ng/mL) at 24 hours after the addition of siRNA or lipoplexes/BLs. ICAM-1 was labeled with anti-mouse ICAM-1 antibody and fluorescein isothiocyanate (FITC)-conjugated secondary antibody (green), and nuclei were counterstained by DAPI (blue). Scale bars, 10 μm. (D,E) Comparison of the suppression of *icam-1* mRNA expression (D) and cell viability (E) obtained by siRNA transfer using Man-PEG$_{2000}$ BLs (1 μg siRNA) and US exposure with that by Lipofectamine 2000. $^*P < 0.05$, $^{**}P < 0.01$ versus no treatment. Each value represents the mean + SD (n = 5). N.T., no treatment.

Statistical Analyses. Results are presented as the mean ± SD of more than three experiments. Analysis of variance was used to test the statistical significance of differences among groups. Two-group comparisons were performed using the Student *t* test and multiple comparisons between control and other groups were performed using the Dunnett's test.

Results

Suppression Effects of ICAM-1 siRNA. The suppression of LPS-induced ICAM-1 expression by ICAM-1 siRNAs (Supporting Fig. 1A) was investigated in primary mouse HECs. As shown in Supporting Fig. 1B, the suppression of ICAM-1 was the highest in ICAM-1 siRNA with sequence 1, and not observed in scrambled siRNA. Therefore, ICAM-1 siRNA containing sequence 1 and scrambled siRNA were used in the following examinations.

Physicochemical Properties of Man-PEG$_{2000}$ BLs. Following enclosure of US imaging gas into Man-PEG$_{2000}$ BLs, lipoplexes became cloudy (data not shown) and the average particle size increased (Supporting Fig. 2A). Following gel electrophoresis experiments, the formation of siRNA complexes in BLs was confirmed (Supporting Fig. 2B). Moreover, ζ-potentials of BLs were lower than that of liposomes (Supporting Fig. 2A), suggesting that siRNA was attached to the surface of cationic bubble liposomes. These physicochemical properties are consistent with our previous reports using plasmid DNA.[23-26]

Intracellular Transport Characteristics of ICAM-1 siRNA. The siRNA transfer efficiency was investigated in primary mouse HECs expressing mannose receptors (Supporting Fig. 4). The amount of siRNA delivered by BLs and US exposure was significantly higher than that by lipoplexes only (Supporting Fig. 3A).

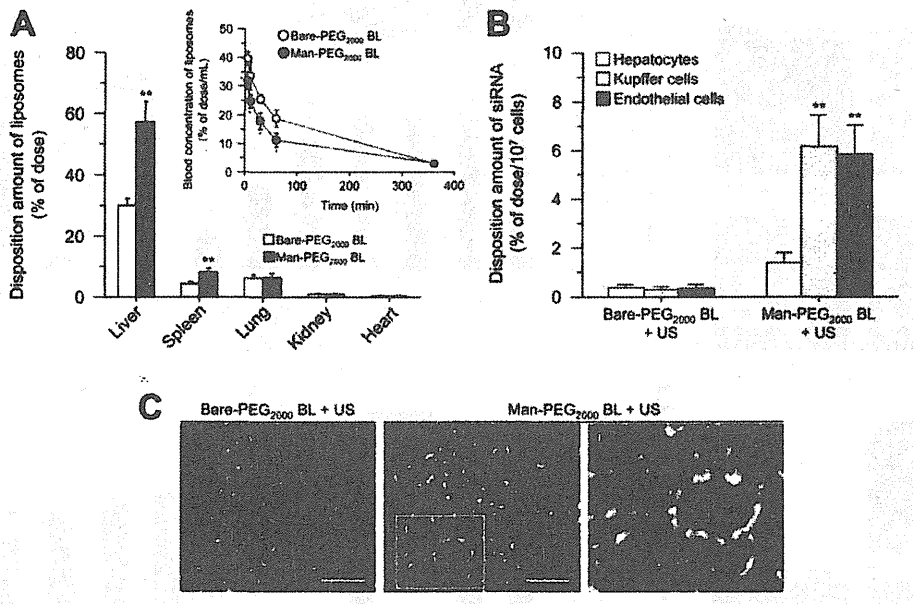

Fig. 2. *In vivo* distribution of ICAM-1 siRNA delivered by Man-PEG_{2000} BLs and US exposure. (A) Tissue distribution and pharmacokinetics of radiolabeled bare- and Man-PEG_{2000} BLs complexed with 10 μg ICAM-1 siRNA after intravenous (iv) administration into mice. Tissue distribution of lipoplexes was measured at 6 hours after iv administration of lipoplexes. Inset shows blood concentration of lipoplexes at predetermined times after iv administration. $*P < 0.05$, $**P < 0.01$ versus the corresponding group of bare-PEG_{2000} lipoplexes. Each value represents the mean ± SD ($n = 5$). (B) Hepatic cellular localization of AlexaFluor-594 labeled ICAM-1 siRNA delivered by bare- and Man-PEG_{2000} BLs (10 μg siRNA) and US exposure at 6 hours after iv administration of lipoplexes into mice. Liver was separated to hepatocytes, Kupffer cells, and endothelial cells by collagenase perfusion, one-step density gradient centrifugation, and magnetic cell sorting as described in the Supporting Materials and Methods. $**P < 0.01$ versus the corresponding group of hepatocytes. Each value represents the mean + SD ($n = 5$). (C) Fluorescent images of hepatic localization of AlexaFluor-594-labeled ICAM-1 siRNA (red) delivered by bare- and Man-PEG_{2000} BLs (10 μg siRNA) and US exposure. HECs were labeled with anti-mouse CD146 antibody and FITC-conjugated secondary antibody (green), and nuclei were counterstained with DAPI (blue). Livers were harvested at 6 hours after iv administration of lipoplexes into mice, and magnified images corresponding to the areas enclosed in boxes are shown in the inset (i). Scale bars, 100 μm.

Moreover, the amount of siRNA delivered by Man-PEG_{2000} BLs and US exposure was higher than unmodified BLs. However, the amount of siRNA was significantly suppressed in the presence of mannan but not suppressed in the presence of chlorpromazine, an endocytosis inhibitor (Supporting Fig. 3B,C). Confocal microscopy analysis of cells after siRNA transfer by bubble lipoplexes with US exposure revealed that siRNA was not colocalized in endosomes (Fig. 1A). These observations suggest that siRNA is directly transferred into the cytoplasm of targeted cells and is not mediated by endocytosis in this siRNA transfer method.

***Suppression Effects of LPS-Induced ICAM-1 Expression* In Vitro.** As shown in Fig. 1B,C, ICAM-1 expression induced by LPS stimulation was suppressed by approximately 80% in siRNA transfer using Man-PEG_{2000} BLs and US exposure. The suppression effect of ICAM-1 expression was not observed for scrambled siRNA. Moreover, this suppression effect was comparable to that by Lipofectamine 2000 (Fig. 1D) but with decreased cytotoxicity (Fig. 1E).

In Vivo *distribution of ICAM-1 siRNA*. We investigated the pharmacokinetic profiles and the tissue distribution of BLs after intravenous administration into mice. Compared with nonmodified BLs, the retention time of Man-PEG_{2000} BLs in the blood was reduced, and localization in both the liver and spleen were increased (Fig. 2A). Moreover, a large amount of ICAM-1 siRNA was distributed in HECs that abundantly express mannose receptors when delivered using Man-PEG_{2000} BLs and US exposure (Fig. 2B,C).

***Suppression Effects of Drug-Induced Hepatic ICAM-1 Expression* In Vivo.** The suppression of ICAM-1 expression by siRNA delivery was investigated in an LPS/D-galactosamine–induced acute hepatitis mouse model (Fig. 3A). As shown in Fig. 3B-D, ICAM-1 mRNA and protein levels in HECs induced by LPS/D-galactosamine stimulation were suppressed by approximately 80% using Man-PEG_{2000} BLs and US exposure. Moreover, ICAM-1 expression induced by CCl_4 and DMN stimulation was also significantly suppressed by the same ICAM-1 siRNA delivery system (Supporting Figs. 6B and 7B). The effects of siRNA dose on ICAM-1 suppression and the duration of ICAM-1 suppression were examined in an LPS/D-galactosamine-induced inflammatory mouse model. Following siRNA delivery using Man-

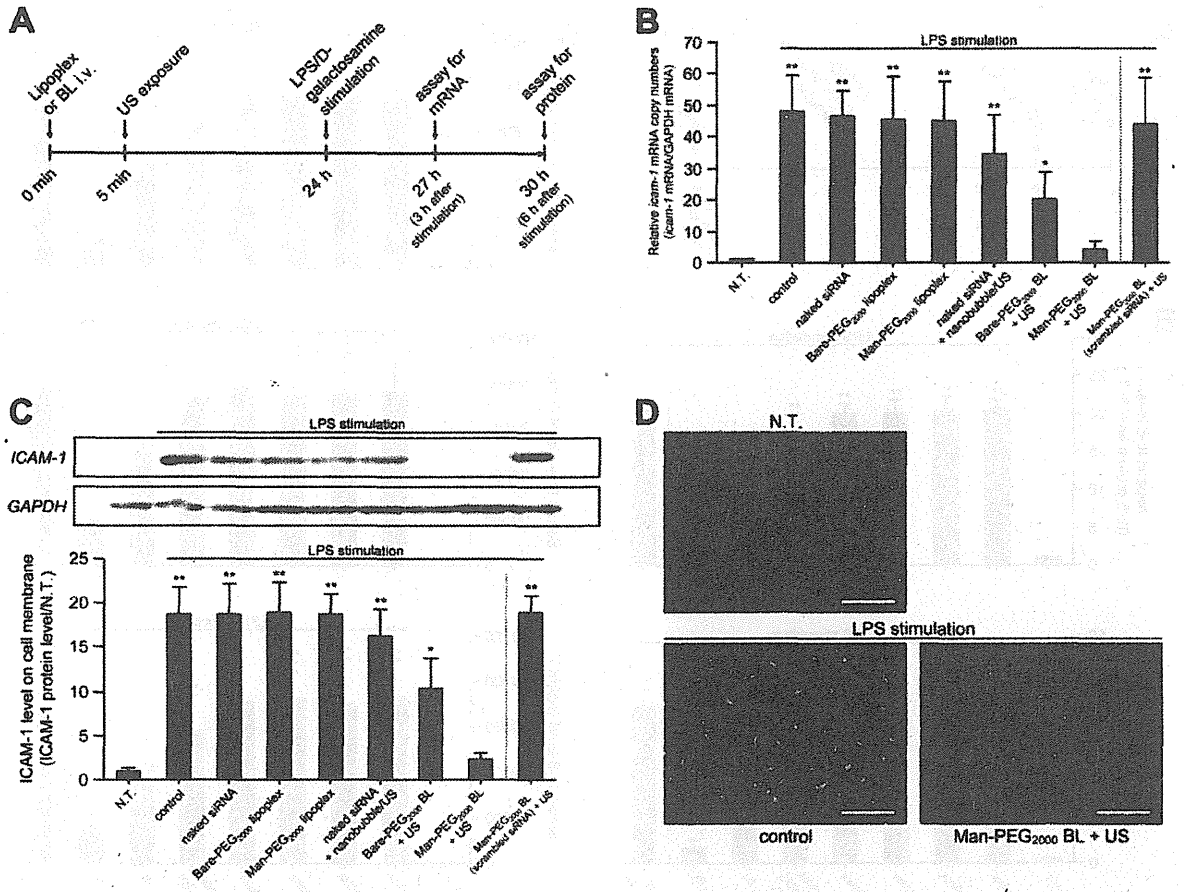

Fig. 3. Suppression effects of ICAM-1 siRNA delivery using Man-PEG_{2000} BLs and US exposure on *icam-1* mRNA and protein expression in HECs of an LPS/D-galactosamine-induced inflammatory mouse model. (A) Evaluation schedule of ICAM-1 expression in LPS/D-galactosamine-stimulated mice. (B-D) The expression level of *icam-1* mRNA in cells (B) and protein on the cell membrane (C, D) obtained by siRNA delivery (10 μg siRNA) using various methods in HECs. At 24 hours after siRNA delivery, LPS/D-galactosamine (1 μg/100 mg/kg) was intraperitoneally administered into mice to induce the acute inflammatory responses. HECs were isolated by collagenase perfusion, one-step density gradient centrifugation, and magnetic cell sorting as described in the Supporting Materials and Methods. The *icam-1* mRNA and protein expression in HECs was determined via quantitative reverse-transcription polymerase chain reaction (B), western blotting/enzyme-linked immunosorbent assay (C), and confocal images (D). The expression levels of mRNA and protein were detected at 3 and 6 hours after LPS/D-galactosamine stimulation, respectively. $^{*}P < 0.05$, $^{**}P < 0.01$ versus no treatment. Each value represents the mean + SD (n = 5). ICAM-1 was labeled with anti-mouse ICAM-1 antibody and FITC-conjugated secondary antibody (green), and nuclei were counterstained with DAPI (blue). Scale bars, 100 μm. N.T., no treatment.

PEG_{2000} BLs and US exposure, suppression was obtained at 10 μg of ICAM-1 siRNA (Supporting Fig. 5A), and was sustained for at least 3 days (Supporting Fig. 5B).

Anti-inflammatory Effects Against Drug-Induced Hepatitis. First, the suppression of leukocyte infiltration by ICAM-1 siRNA delivery was evaluated in an LPS/D-galactosamine–induced inflammatory mouse model (Fig. 4A). As shown in Fig. 4B,D, the expression of interleukin (IL)-8 and monocyte chemotactic protein 1 (MCP-1) was suppressed, and a significantly decreased number of infiltrated leukocytes were detected after siRNA delivery using Man-PEG_{2000} BLs and US exposure. Moreover, the production of proinflammatory cytokines (tumor necrosis factor α [TNF-α], interferon-γ [IFN-γ], and IL-6) were also suppressed by this siRNA delivery (Fig. 4C).

The anti-inflammatory effects obtained by ICAM-1 siRNA delivery were investigated next. As shown in Fig. 5A, alanine aminotransferase (ALT)/aspartate aminotransferase (AST) activities in the serum were markedly suppressed by siRNA delivery using Man-PEG_{2000} BLs and US exposure (Fig. 5A). As shown in Fig. 5B, hepatic apoptosis induced by LPS/D-galactosamine stimulation was significantly suppressed by this ICAM-1 siRNA delivery. Moreover, we performed hematoxylin and eosin (H&E) staining of liver sections to evaluate the effects on hepatic structural features. Although the circular and tube formations of the hepatic central vein were observed in normal liver section (Fig. 5C, left), they were crushed in the LPS-stimulated liver section (Fig. 5C, middle). On the other hand, destruction of the hepatic central vein induced by

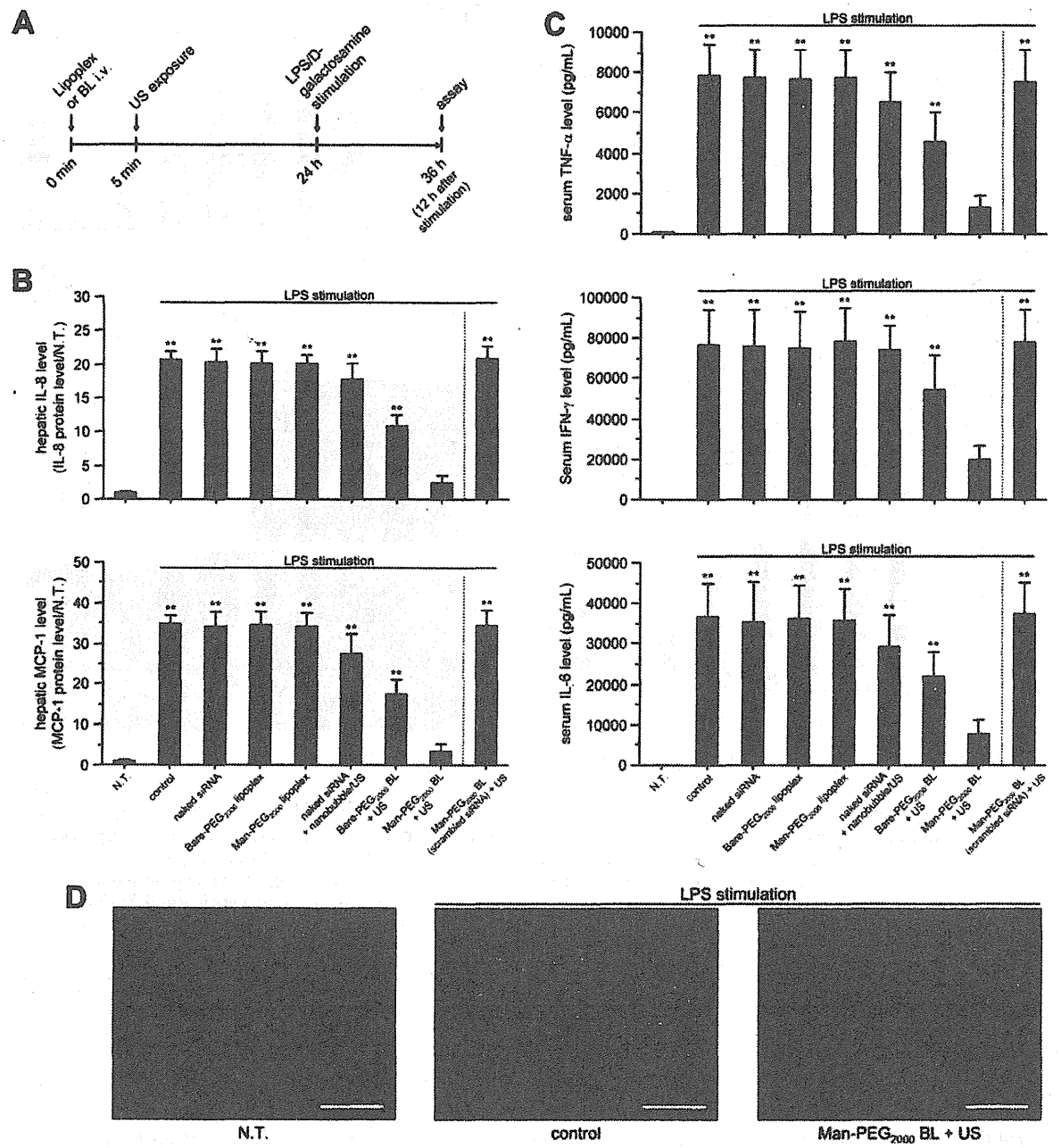

Fig. 4. Suppression effects of ICAM-1 siRNA delivery using Man-PEG_{2000} BLs and US exposure on leukocyte infiltration and proinflammatory cytokine production in an LPS/D-galactosamine-induced inflammatory mouse model. (A) Evaluation schedule of leukocyte infiltration and proinflammatory cytokine production in LPS/D-galactosamine-stimulated mice. (B,C) Levels of IL-8 and MCP-1 expression in the liver (B) and the levels of TNF-α, IFN-γ, and IL-6 secretion in the serum (C) after siRNA delivery (10 μg siRNA) using various delivery methods 12 hours after LPS/D-galactosamine stimulation. $^{**}P < 0.01$ versus no treatment. Each value represents the mean + SD (n = 5). N.T., no treatment. (D) Photomicrographs of infiltrated leukocytes after siRNA delivery using Man-PEG_{2000} BLs (10 μg siRNA) and US exposure in LPS/D-galactosamine-stimulated mouse liver. Leukocytes were labeled with anti-mouse Gr-1 (Ly-6G) antibody and rhodamine isothiocyanate-conjugated secondary antibody (red), and nuclei were counterstained with DAPI (blue). Scale bars, 100 μm. $^{**}P < 0.01$ versus no treatment. Each value represents the mean + SD (n = 5). N.T., no treatment.

LPS stimulation was significantly suppressed by ICAM-1 siRNA delivery using Man-PEG_{2000} BLs and US exposure (Fig. 5C, right), suggesting that the liver injury induced by LPS-stimulation is suppressed by this siRNA delivery. Similar effects by this ICAM-1 siRNA delivery were also observed for CCl_4- and DMN-induced inflammatory mouse models (Supporting Figs. 6C,D and 7C,D).

Anti-inflammatory Effects Against IR-Induced Liver Injury. The effects of ICAM-1 suppression by delivery of siRNA was evaluated for IR-induced liver

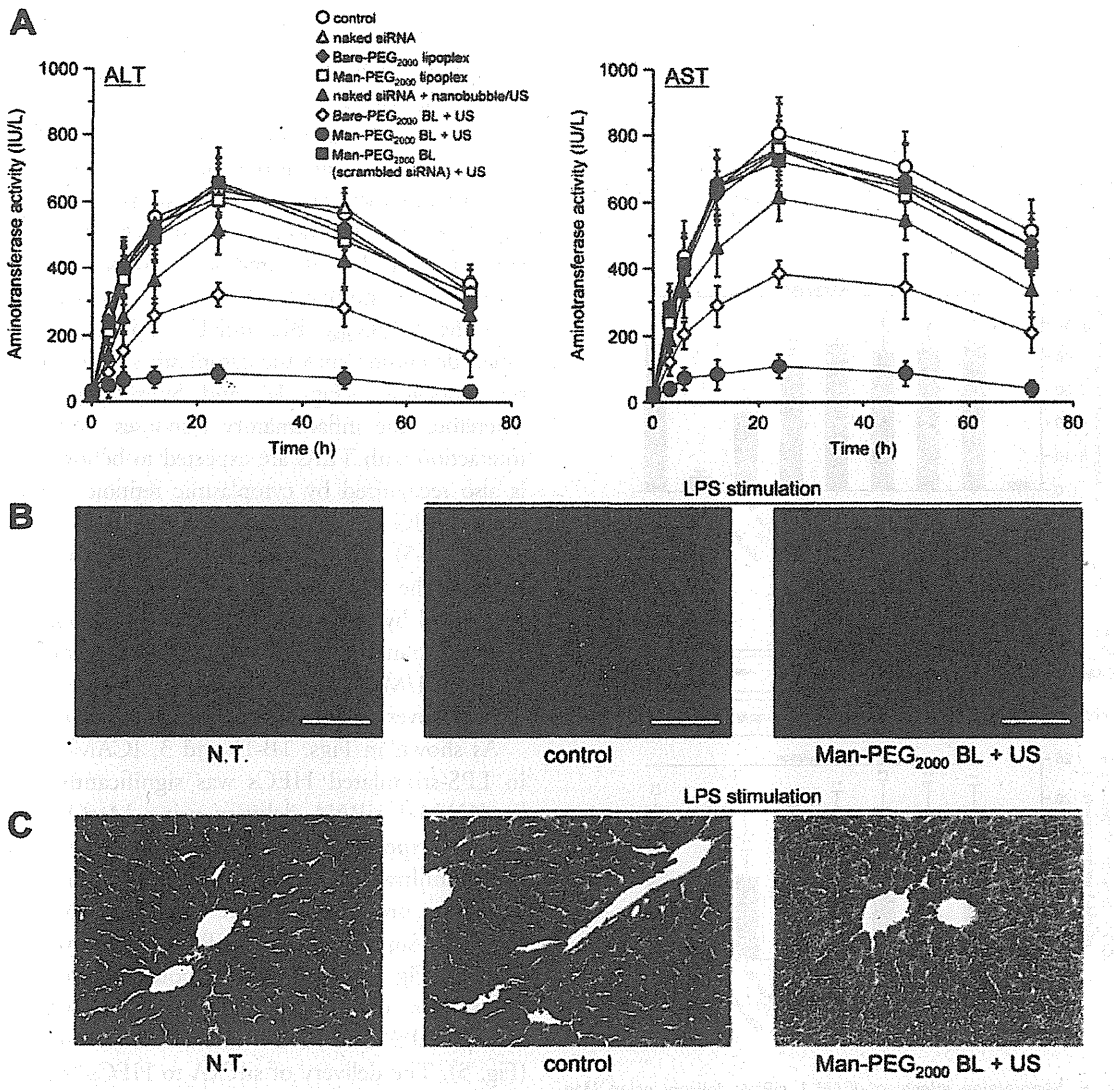

Fig. 5. Suppression effects of ICAM-1 siRNA delivery using Man-PEG_{2000} BLs and US exposure on liver toxicity in an LPS/D-galactosamine-induced inflammatory mouse model. (A) The level of serum ALT/AST activities after siRNA delivery (10 μg siRNA) using various methods at predetermined times after LPS/D-galactosamine stimulation. Each value represents the mean ± SD (n = 5). (B) Fluorescent images of apoptosis after siRNA delivery using Man-PEG_{2000} BLs (10 μg siRNA) and US exposure in LPS/D-galactosamine-stimulated mice. Apoptosis (green) was detected via terminal deoxynucleotidyl transferase-mediated deoxyuridine triphosphate nick-end labeling, and nuclei were counterstained with DAPI (blue). Scale bars, 100 μm. (C) Liver histology with H&E staining 24 hours after siRNA delivery using Man-PEG_{2000} BLs (10 μg siRNA) and US exposure in LPS/D-galactosamine-induced inflammatory mouse model. Black arrows: destruction of tube formation in hepatic central vein. Scale bars, 100 μm.

injury (Fig. 6A). As shown in Fig. 6B,C, ICAM-1 expression induced by IR stimulation was suppressed by siRNA delivery using Man-PEG_{2000} BLs and US exposure. Moreover, IL-8/MCP-1 expression and proinflammatory cytokine production were also suppressed (Fig. 7B,C). Following the examination of liver toxicity, ALT/AST activities in the serum and hepatic apoptosis were significantly suppressed (Fig. 8A,B). Moreover, after H&E staining of liver sections, the circular and tube formations of hepatic central vein in the normal liver (Fig. 8C, left) section is destructed by IR stimulation (Fig. 8C, middle), on the other hand, IR-derived destruction of hepatic central vein was suppressed by this ICAM-1 siRNA delivery (Fig. 5C, right).

Discussion

In the sonoporation method, transient pores are created on the cell membrane followed by the destruction of microbubbles, and a large amount of nucleic acids can be directly transferred into the cytoplasm.[21,26,27] Because siRNA is functionalized in the cytoplasm, gene

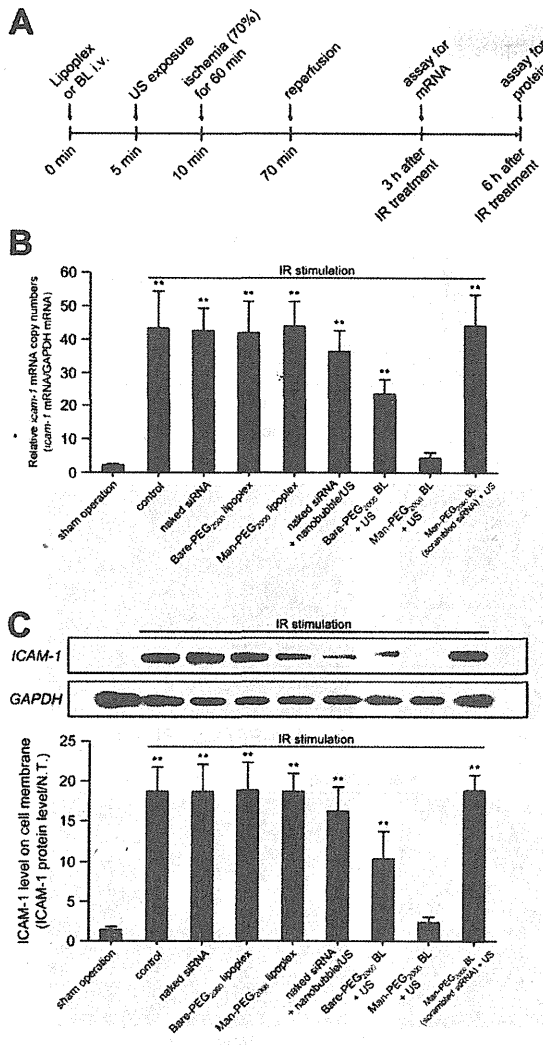

Fig. 6. Suppression effects of ICAM-1 siRNA delivery using Man-PEG_{2000} BLs and US exposure on *icam-1* mRNA and protein expression in HECs of an IR-induced hepatic inflammatory mouse model. (A) Evaluation schedule of ICAM-1 expression in hepatic IR-stimulated mice. (B,C) Expression level of *icam-1* mRNA in cells (B) and protein on the cell membrane (C) obtained by siRNA delivery (10 μg siRNA) using various delivery methods in HECs. HECs were isolated via collagenase perfusion, one-step density gradient centrifugation, and magnetic cell sorting as described in the Supporting Materials and Methods. The *icam-1* mRNA and protein expression in HECs was determined via quantitative reverse-transcription polymerase chain reaction (B) and western blotting/enzyme-linked immunosorbent assay (C). Expression levels of mRNA and protein were detected at 3 and 6 hours after IR stimulation, respectively. $*P < 0.05$, $**P < 0.01$ versus sham operation. Each value represents the mean + SD ($n = 5$).

transfer using Man-PEG_{2000} BLs and US exposure[23-26] would be also suitable for siRNA delivery. In the present study, we applied this gene transfer method for the selective and efficient delivery of siRNA to HECs *in vivo* and investigated the anti-inflammatory effects in various types of inflammatory responses.

The innate inflammatory responses based on the interaction with siRNA and Toll-like receptor (TLR)-3, -7, and -8 should be excluded for evaluating the gene suppression effects of siRNA, but should be considered for clinical applications of siRNA.[28,29] The proinflammatory cytokines (such as TNF-α, IFN-γ, and IL-6) can be induced by siRNA interaction with endosomal TLR-3, -7, and -8 in siRNA transfer using conventional nonviral carriers.[28,29] Transfer of siRNA using Man-PEG_{2000} BLs and US exposure results in the direct deposition into the cytoplasm and is not mediated by endocytosis (Fig. 1A and Supporting Fig. 3C).[26] Therefore, the inflammatory responses followed by the interaction with TLRs are expected to be low, but siRNA is also recognized by cytoplasmic retinoic acid-inducible gene 1 (RIG-1)/melanoma differentiation-associated gene 5 (MDA-5) involved in inflammatory responses.[28,30] Because the modification of 3′-overhang sequences is suppressed by the activation of interferon-responsive factors 3/7, transcriptional factors that exist downstream of the RIG-1/MDA-5 pathway,[31,32] we used siRNAs with 3′-dTdT overhang sequences (Supporting Fig. 1A).

As shown in Figs. 1B-D and 3, ICAM-1 expression in LPS-stimulated HECs was significantly suppressed by ICAM-1 siRNA delivery using Man-PEG_{2000} BLs and US exposure, both *in vitro* and *in vivo*. Similarly, tissue infiltration of leukocytes and proinflammatory cytokine production were both suppressed after ICAM-1 suppression by siRNA delivery using this method (Fig. 4). Furthermore, potent anti-inflammatory effects were obtained by this ICAM-1 siRNA delivery in an LPS-stimulated inflammatory mouse model (Fig. 5). The delivery of siRNA to HECs, which express mannose receptors (Supporting Fig. 4),[33] was selective and efficient using Man-PEG_{2000} BLs with US exposure (Fig. 2B,C). Moreover, because a large amount of siRNA was directly transferred into the cytoplasm (Fig. 1A and Supporting Fig. 3C),[26] endosomal escape and degradation within endosomes could be evaded. These data may indicate that nucleic acid transfer using Man-PEG_{2000} BLs and US exposure can be applied for siRNA delivery.

Although LPS is widely used to evaluate the induction of acute inflammatory responses, they are induced by not only various medicines but also surgical operations.[34] Aiming for the clinical application of anti-inflammatory therapy using our siRNA delivery method, the anti-inflammatory effects against various inflammatory models in mice were investigated. After evaluation of the anti-inflammatory effects against CCl_4-, DMN-, and IR-stimulated inflammation, ICAM-1 expression in HECs and the inflammatory responses was significantly suppressed by ICAM-1

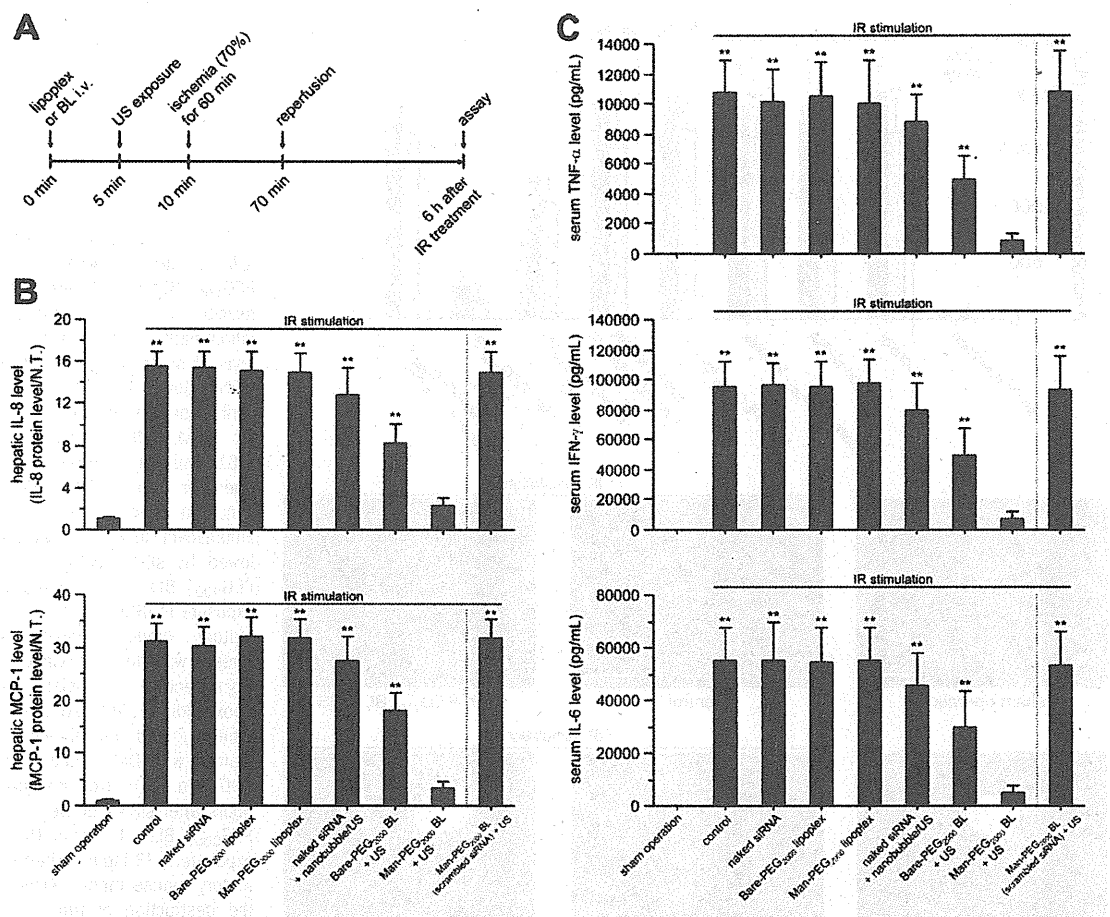

Fig. 7. Suppression effects of ICAM-1 siRNA delivery using Man-PEG_{2000} BLs and US exposure on leukocyte infiltration and proinflammatory cytokine production in IR-induced hepatic inflammatory mouse model. (A) Evaluation schedule of leukocyte infiltration and proinflammatory cytokine production in hepatic IR-stimulated mice. (B,C) Levels of IL-8 and MCP-1 expression in the liver (B) and TNF-α, IFN-γ, IL-6 secretion in the serum (C) after siRNA delivery (10 μg siRNA) using various delivery methods 6 hours after IR stimulation. $^{**}P < 0.01$ versus sham operation. Each value represents the mean + SD (n = 5).

siRNA delivery using Man-PEG_{2000} BLs and US exposure in these inflammatory mouse models (Figs. 6-8 and Supporting Figs. 6 and 7). Although the mechanisms of inflammatory responses as a result of LPS, CCl_4, DMN, and IR stimulation are different,[5,6,35,36] ICAM-1 expression in HECs is reported in various types of inflammation, including drug-induced hepatic inflammation and IR-induced liver injury.[7] These data suggest that anti-inflammatory effects obtained by ICAM-1 siRNA delivery using Man-PEG_{2000} BLs and US exposure may be beneficial for acute hepatitis and liver injury.

In the present study, efficient ICAM-1 suppression was obtained at a dose of 1 μg siRNA/mouse (0.05 mg/kg) for siRNA delivery using Man-PEG_{2000} BLs and US exposure *in vivo* (Supporting Fig. 5A). This dose of siRNA is lower than those reported for other studies evaluating the therapeutic effects using siRNA, although the therapeutic mechanism and delivery methods of each siRNA are likely to be different.[37-39] These findings suggest that the increased distribution of siRNA into HECs by mannose modification (Fig. 2) and the enhancement of intracytoplasmic siRNA transfer by sonoporation (Fig. 1A and Supporting Fig. 3) could contribute to the potent anti-inflammatory effects observed at a low dose of siRNA in our siRNA delivery method.

ICAM-1 suppression effects were only sustained for 72 hours by siRNA delivery using Man-PEG_{2000} BLs and US exposure (Supporting Fig. 5B). However, because the disease target of this study was acute inflammation, the potent therapeutic effects might be obtained in short duration and single administration of siRNA. Recently, it has been reported that ICAM-1 is involved in various diseases not only for acute/chronic hepatic failure, but also Crohn's disease, ulcerative colitis, and ileus.[40-42] In addition, antisense oligonucleotides against ICAM-1 (ISIS-2302; Alicaforsen)

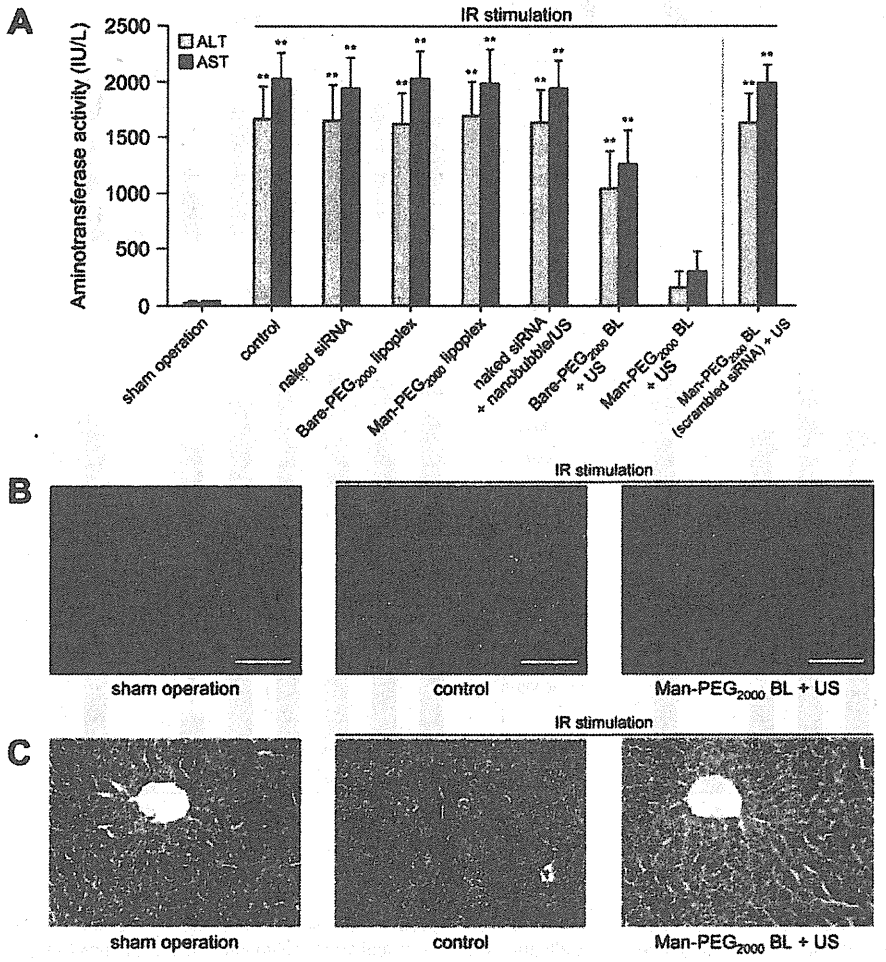

Fig. 8. Suppression effects of ICAM-1 siRNA delivery using Man-PEG_{2000} BLs and US exposure on liver toxicity in an IR-induced hepatic inflammatory mouse model. (A) The level of serum ALT/AST activities after siRNA delivery (10 μg siRNA) using various delivery methods 24 hours after hepatic IR stimulation. $^{**}P < 0.01$versus the corresponding sham operation group. Each value represents the mean + SD (n = 5). (B) Fluorescent images of apoptosis followed by siRNA delivery using Man-PEG_{2000} BLs (10 μg siRNA) and US exposure in IR-induced hepatic inflammatory mouse model. Apoptosis (green) was detected via terminal deoxynucleotidyl transferase-mediated deoxyuridine triphosphate nick-end labeling, and nuclei were counterstained with DAPI (blue). Scale bars, 100 μm. (C) Liver histology at 24 hours after siRNA delivery using Man-PEG_{2000} BLs (10 μg siRNA) and US exposure in IR-induced hepatic inflammatory mouse model. Arrows indicate the destruction of tube formation in the hepatic central vein. Scale bars, 100 μm.

are currently under development for the treatment of Crohn's disease and ulcerative colitis.[43,44] However, most of these inflammatory diseases are based on chronic inflammation. In the present study, it is strongly suggested that transfer of ICAM-1 siRNA using Man-PEG_{2000} BLs and US exposure enables a large amount of siRNA to be delivered the cytoplasm of targeted cells (Fig. 1A and Supporting Fig. 3). Therefore, to prolong the duration of gene suppression using this siRNA delivery system, future studies using cholesterol-modified siRNA[45] or locked nucleic acid,[46] which are forms of stable siRNA resistant to enzymatic degradation, might be necessary for application to a variety of chronic inflammatory diseases.

In conclusion, ICAM-1 siRNA was transferred into HECs selectively and efficiently, and sufficient ICAM-1 suppression effects were obtained by ICAM-1 siRNA transfer using Man-PEG_{2000} BLs and US exposure, both *in vitro* and *in vivo*. Moreover, potent anti-inflammatory effects were achieved against various types of inflammation by this ICAM-1 siRNA transfer. These findings contribute to overcoming the poor efficiency of siRNA transfer into the cytoplasm of the targeted cells using nonviral carriers, and this novel siRNA delivery method using Man-PEG_{2000} BLs and US exposure may offer a valuable system for medical treatment where the cellular targets are HECs.

References

1. Verma S, Kaplowitz N. Diagnosis, management and prevention of drug-induced liver injury. Gut 2009;58:1555-1564.
2. Gurusamy KS, Gonzalez HD, Davidson BR. Current protective strategies in liver surgery. World J Gastroenterol 2010;16:6098-6103.
3. Freeman AJ, Dore GJ, Law MG, Thorpe M, Von Overbeck J, Lloyd AR, et al. Estimating progression to cirrhosis in chronic hepatitis C virus infection. HEPATOLOGY 2001;34:809-816.
4. Kuper H, Ye W, Broomé U, Romelsjö A, Mucci LA, Ekbom A, et al. The risk of liver and bile duct cancer in patients with chronic viral hepatitis, alcoholism, or cirrhosis. HEPATOLOGY 2001;34:714-718.
5. Tsuchiya H, Kaibori M, Yanagida H, Yokoigawa N, Kwon AH, Okumura T, et al. Pirfenidone prevents endotoxin-induced liver injury after partial hepatectomy in rats. J Hepatol 2004;40:94-101.
6. Teoh NC, Farrell GC. Hepatic ischemia reperfusion injury: pathogenic mechanisms and basis for hepatoprotection. J Gastroenterol Hepatol 2003;18:891-902.

7. Jaeschke H. Mechanisms of liver injury. II. Mechanisms of neutrophil-induced liver cell injury during hepatic ischemia-reperfusion and other acute inflammatory conditions. Am J Physiol Gastrointest Liver Physiol 2006;290:1083-1088.
8. Rijcken E, Krieglstein CF, Anthoni C, Laukoetter MG, Mennigen R, Spiegel HU, et al. ICAM-1 and VCAM-1 antisense oligonucleotides attenuate in vivo leucocyte adherence and inflammation in rat inflammatory bowel disease. Gut 2002;51:529-535.
9. Kono H, Uesugi T, Froh M, Rusyn I, Bradford BU, Thurman RG. ICAM-1 is involved in the mechanism of alcohol-induced liver injury: studies with knockout mice. Am J Physiol Gastrointest Liver Physiol 2001;280:G1289-G1295.
10. Elbashir SM, Lendeckel W, Tuschl T. RNA interference is mediated by 21- and 22-nucleotide RNAs. Genes Dev 2001;15:188-200.
11. Elbashir SM, Harborth J, Lendeckel W, Yalcin A, Weber K, Tuschl T. Duplexes of 21-nucleotide RNAs mediate RNA interference in cultured mammalian cells. Nature 2001;411:494-498.
12. Sato A, Takagi M, Shimamoto A, Kawakami S, Hashida M. Small interfering RNA delivery to the liver by intravenous administration of galactosylated cationic liposomes in mice. Biomaterials 2007;28:1434-1442.
13. Kawakami S, Hashida M. Targeted delivery systems of small interfering RNA by systemic administration. Drug Metab Pharmacokinet 2007;22:142-151.
14. Mok H, Lee SH, Park JW, Park TG. Multimeric small interfering ribonucleic acid for highly efficient sequence-specific gene silencing. Nat Mater 2010;9:272-278.
15. Kim SS, Ye C, Kumar P, Chiu I, Subramanya S, Wu H, et al. Targeted delivery of siRNA to macrophages for anti-inflammatory treatment. Mol Ther 2010;18:993-1001.
16. Davis ME, Zuckerman JE, Choi CH, Seligson D, Tolcher A, Alabi CA, et al. Evidence of RNAi in humans from systemically administered siRNA via targeted nanoparticles. Nature 2010;464:1067-1070.
17. Takemoto H, Ishii A, Miyata K, Nakanishi M, Oba M, Ishii T, et al. Polyion complex stability and gene silencing efficiency with a siRNA-grafted polymer delivery system. Biomaterials 2010;31:8097-8105.
18. Higuchi Y, Kawakami S, Hashida M. Strategies for in vivo delivery of siRNAs: recent progress. BioDrugs 2010;24:195-205.
19. Hernot S, Klibanov AL. Microbubbles in ultrasound-triggered drug and gene delivery. Adv Drug Deliv Rev 2008;60:1153-1166.
20. Li YS, Davidson E, Reid CN, McHale AP. Optimising ultrasound-mediated gene transfer (sonoporation) in vitro and prolonged expression of a transgene in vivo: potential applications for gene therapy of cancer. Cancer Lett 2009;273:62-69.
21. Lentacker I, Wang N, Vandenbroucke RE, Demeester J, De Smedt SC, Sanders NN. Ultrasound exposure of lipoplex loaded microbubbles facilitates direct cytoplasmic entry of the lipoplexes. Mol Pharm 2009;6:457-467.
22. Negishi Y, Matsuo K, Endo-Takahashi Y, Suzuki K, Matsuki Y, Takagi N, et al. Delivery of an angiogenic gene into ischemic muscle by novel bubble liposomes followed by ultrasound exposure. Pharm Res 2011; 28:712-719.
23. Un K, Kawakami S, Suzuki R, Maruyama K, Yamashita F, Hashida M. Development of an ultrasound-responsive and mannose-modified gene carrier for DNA vaccine therapy. Biomaterials 2010;31:7813-7826.
24. Un K, Kawakami S, Suzuki R, Maruyama K, Yamashita F, Hashida M. Suppression of melanoma growth and metastasis by DNA vaccination using an ultrasound-responsive and mannose-modified gene carrier. Mol Pharm 2011;8:543-554.
25. Un K, Kawakami S, Higuchi Y, Suzuki R, Maruyama K, Yamashita F, et al. Involvement of activated transcriptional process in efficient gene transfection using unmodified and mannose-modified bubble lipoplexes with ultrasound exposure. J Control Release 2011;156:355-363.
26. Un K, Kawakami S, Yoshida M, Higuchi Y, Suzuki R, Maruyama K, et al. The elucidation of gene transferring mechanism by ultrasound-responsive unmodified and mannose-modified lipoplexes. Biomaterials 2011;32:4659-4669.
27. Negishi Y, Endo Y, Fukuyama T, Suzuki R, Takizawa T, Omata D, et al. Delivery of siRNA into the cytoplasm by liposomal bubbles and ultrasound. J Control Release 2008;132:124-130.
28. Matsushima H, Yamada N, Matsue H, Shimada S. TLR3-, TLR7-, and TLR9-mediated production of proinflammatory cytokines and chemokines from murine connective tissue type skin-derived mast cells but not from bone marrow-derived mast cells. J Immunol 2004;173:531-541.
29. Kawai T, Akira S. Toll-like receptor and RIG-I-like receptor signaling. Ann N Y Acad Sci 2008;1143:1-20.
30. Matsukura S, Kokubu F, Kurokawa M, Kawaguchi M, Ieki K, Kuga H, et al. Role of RIG-I, MDA-5, and PKR on the expression of inflammatory chemokines induced by synthetic dsRNA in airway epithelial cells. Int Arch Allergy Immunol 2007;143:80-83.
31. Marques JT, Devosse T, Wang D, Zamanian-Daryoush M, Serbinowski P, Hartmann R, et al. A structural basis for discriminating between self and nonself double-stranded RNAs in mammalian cells. Nat Biotechnol 2006;24:559-565.
32. Sato Y, Murase K, Kato J, Kobune M, Sato T, Kawano Y, et al. Resolution of liver cirrhosis using vitamin A-coupled liposomes to deliver siRNA against a collagen-specific chaperone. Nat Biotechnol 2008;26: 431-442.
33. Elvevold K, Simon-Santamaria J, Hasvold H, McCourt P, Smedsrød B, Sørensen KK. Liver sinusoidal endothelial cells depend on mannose receptor-mediated recruitment of lysosomal enzymes for normal degradation capacity. HEPATOLOGY 2008;48:2007-2015.
34. Norris W, Paredes AH, Lewis JH. Drug-induced liver injury in 2007. Curr Opin Gastroenterol 2008;24:287-297.
35. Simeonova PP, Gallucci RM, Hulderman T, Wilson R, Kommineni C, Rao M, et al. The role of tumor necrosis factor-alpha in liver toxicity, inflammation, and fibrosis induced by carbon tetrachloride. Toxicol Appl Pharmacol 2001;177:112-120.
36. Oyaizu T, Shikata N, Senzaki H, Matsuzawa A, Tsubura A. Studies on the mechanism of dimethylnitrosamine-induced acute liver injury in mice. Exp Toxicol Pathol 1997;49:375-380.
37. Song E, Lee SK, Wang J, Ince N, Ouyang N, Min J, et al. RNA interference targeting Fas protects mice from fulminant hepatitis. Nat Med 2003;9:347-351.
38. Yano J, Hirabayashi K, Nakagawa S, Yamaguchi T, Nogawa M, Kashimori I, et al. Antitumor activity of small interfering RNA/cationic liposome complex in mouse models of cancer. Clin Cancer Res 2004;10: 7721-7726.
39. Zimmermann TS, Lee AC, Akinc A, Bramlage B, Bumcrot D, Fedoruk MN, et al. RNAi-mediated gene silencing in non-human primates. Nature 2006;441:111-114.
40. Yacyshyn BR, Schievella A, Sewell KL, Tami JA. Gene polymorphisms and serological markers of patients with active Crohn's disease in a clinical trial of antisense to ICAM-1. Clin Exp Immunol 2005;141:141-147.
41. Miner PB Jr, Geary RS, Matson J, Chuang E, Xia S, Baker BF, et al. Bioavailability and therapeutic activity of alicaforsen (ISIS 2302) administered as a rectal retention enema to subjects with active ulcerative colitis. Aliment Pharmacol Ther 2006;23:1427-1434.
42. The FO, Jonge WJ, Bennink RJ, van den Wijngaard RM, Boeckxstaens GE. The ICAM-1 antisense oligonucleotide ISIS-3082 prevents the development of postoperative ileus in mice. Br J Pharmacol 2005;146: 252-258.
43. Yacyshyn BR, Chey WY, Goff J, Salzberg B, Baerg R, Buchman AL, et al. Double blind, placebo controlled trial of the remission inducing and steroid sparing properties of an ICAM-1 antisense oligodeoxynucleotide, alicaforsen (ISIS 2302), in active steroid dependent Crohn's disease. Gut 2002;51:30-36.
44. van Deventer SJ, Tami JA, Wedel MK. A randomised, controlled, double blind, escalating dose study of alicaforsen enema in active ulcerative colitis. Gut 2004;53:1646-1651.
45. Ambardekar VV, Han HY, Varney ML, Vinogradov SV, Singh RK, Vetro JA. The modification of siRNA with 3′ cholesterol to increase nuclease protection and suppression of native mRNA by select siRNA polyplexes. Biomaterials 2011;32:1404-1411.
46. Elmén J, Thonberg H, Ljungberg K, Frieden M, Westergaard M, Xu Y, et al. Locked nucleic acid (LNA) mediated improvements in siRNA stability and functionality. Nucleic Acids Res 2005;33:439-447.

Journal of Controlled Release 160 (2012) 362–366

Contents lists available at SciVerse ScienceDirect

Journal of Controlled Release

journal homepage: www.elsevier.com/locate/jconrel

Prophylactic immunization with Bubble liposomes and ultrasound-treated dendritic cells provided a four-fold decrease in the frequency of melanoma lung metastasis

Yusuke Oda [a,1], Ryo Suzuki [a,1], Shota Otake [a,1], Norihito Nishiie [a], Keiichi Hirata [a], Risa Koshima [a], Tetsuya Nomura [a], Naoki Utoguchi [a], Nobuki Kudo [b], Katsuro Tachibana [c], Kazuo Maruyama [a,*]

[a] Department of Biopharmaceutics, School of Pharmaceutical Sciences, Teikyo University, Japan
[b] Laboratory of Biomedical Engineering, Graduate School of Information Science and Technology, Hokkaido University, Japan
[c] Department of Anatomy, School of Medicine, Fukuoka University, Japan

ARTICLE INFO

Article history:
Received 15 July 2011
Accepted 6 December 2011
Available online 13 December 2011

Keywords:
Dendritic cells
Antigen delivery system
Cancer immunotherapy
Ultrasound
Liposomes

ABSTRACT

Melanoma has an early tendency to metastasize, and the majority of the resulting deaths are caused by metastatic melanoma. It is therefore important to develop effective therapies for metastasis. Dendritic cell (DC)-based cancer immunotherapy has been proposed as an effective therapeutic strategy for metastasis and recurrence due to prime tumor-specific cytotoxic T lymphocytes. In this therapy, it is important that DCs present peptides derived from tumor-associated antigens on MHC class I molecules. Previously, we developed an innovative approach capable of directly delivering exogenous antigens into the cytosol of DCs using perfluoropropane gas-entrapping liposomes (Bubble liposomes, BLs) and ultrasound. In the present study, we investigated the prevention of melanoma lung metastasis via DC-based immunotherapy. Specifically, antigens were extracted from melanoma cells and used to treat DCs by BL and ultrasound. Delivery into the DCs by this route did not require the endocytic pathway. The delivery efficiency was approximately 74.1%. DCs treated with melanoma-derived antigens were assessed for *in vivo* efficacy in a mouse model of lung metastasis. Prophylactic immunization with BL/ultrasound-treated DCs provided a four-fold decrease in the frequency of melanoma lung metastases. These *in vitro* and *in vivo* results demonstrate that the combination of BLs and ultrasound is a promising method for antigen delivery system into DCs.

1. Introduction

Melanoma is the most devastating form of skin cancer and represents a leading cause of cancer death. Relative to the tumor mass, melanomas have an early tendency to metastasize; indeed, the majority of melanoma deaths are caused by metastatic disease. As a result, the prognosis for melanoma is poor. In fact, the 5-year survival rate of patients with localized melanoma is up to 90%; in contrast, patients with metastasized melanoma have 5-year survival rates of only 20% [1,2]. Additionally, melanoma is usually resistant to standard chemotherapy, and the response rate for any single agent or combination of agents ranges from 5% to 45% [3,4]. Based on these data, there is a clear need to develop effective therapy for metastasized melanoma. There are various therapeutic methods for metastatic cancer, such as surgical treatment, chemotherapy, radiotherapy, and immunotherapy. Of these methods, immunotherapy may be the most promising because of the possibility of preventing systemic metastasis and recurrence in the long term [5–9].

Dendritic cells (DCs), which are unique antigen-presenting cells capable of priming naive T cells, have been used as vaccine carriers for cancer immunotherapy [6,10]. To induce an effective tumor-specific cytotoxic T-lymphocyte (CTL) response, DCs should abundantly present epitope peptides derived from tumor-associated antigens (TAAs) via major histocompatibility complex (MHC) class I molecules and MHC class II molecules [11]. In general, exogenous antigens (such as TAAs in DCs) are preferentially presented on MHC class II molecules [12,13]. On the other hand, the majority of peptides presented via the MHC class I molecules are generated from endogenously synthesized proteins that are degraded by the proteasome [12]. Therefore, in order to efficiently prime TAA-specific CTLs, it is necessary to develop a novel antigen delivery system that can induce MHC class I-restricted TAA presentation on DCs. Several researchers have studied antigen delivery tools based on the cross-presentation theory of exogenous antigens in DCs [14–19]. Proposed antigen delivery carriers have included liposomes [15,16], poly(γ-glutamic acid) nanoparticles [17], and cholesterol pullulan nanoparticles [18]. All of these carriers deliver the antigens into DCs via the endocytic pathway, inducing the leaking of exogenous antigens from the endosome into the cytosol. Finally, it is thought that the antigens leaked into the cytosol are

Abbreviations: BL, Bubble liposome; CTL, cytotoxic T-lymphocyte; DC, dendritic cell; FITC, fluorescein isothiocyanate; MHC, major histocompatibility complex; MW, molecular weight; PBS, phosphate-buffered saline; TAA, tumor-associated antigen; US, ultrasound.

* Corresponding author at: Department of Biopharmaceutics, School of Pharmaceutical Sciences, Teikyo University, 1091-1 Suwarashi, Midori-ku, Sagamihara, Kanagawa 252-5195, Japan. Tel.: +81 42 685 3722; fax: +81 42 685 3432.
E-mail address: maruyama@pharm.teikyo-u.ac.jp (K. Maruyama).
[1] These authors contributed equally to this work.

0168-3659/$ – see front matter.
doi:10.1016/j.jconrel.2011.12.003

presented on MHC class I molecules. As an alternative, we have sought to use an antigen delivery system that does not rely on the endocytic pathway.

Multiple papers have reported the use of microbubbles for ultrasound-mediated gene and drug delivery [20–26]. In this delivery system, microstreams and microjets, which are induced by disruption of nano/microbubbles exposed to ultrasound, promote the transfer of extracellular materials into cells by opening transient pores in the cell membrane [27,28]. Previously, we described ultrasound-mediated antigen delivery in DCs using Bubble liposomes (BLs) containing perfluoropropane, an ultrasound imaging gas [29]. Using this system, a model antigen (ovalbumin) could be delivered into the cytosol of DCs independent of the endocytic pathway. This technique provided direct entry of the exogenous antigens into the MHC class I presentation pathway, resulting in the priming of exogenous antigen-specific CTLs. We proposed that this system could facilitate the delivery of crude antigens (such as tumor lysates and extracts) because such substrates could enter cells via a transient pore. In the present study, we used fluorescein isothiocyanate (FITC)-dextran as a substrate to characterize antigen delivery by BLs and ultrasound. Additionally, we assessed the possible application of BLs and ultrasound in DC-based immunotherapy in an *in vivo* model of melanoma. Specifically, we delivered tumor-extracted antigens into DCs using BLs and ultrasound, and investigated whether these treated DCs protected mice from lung metastasis.

2. Materials and methods

2.1. Cells

B16/BL6 cells, a C57BL/6-derived melanoma cell line, were cultured in RPMI 1640 (Sigma Co., St. Louis, MO, USA) supplemented with 10% heat inactivated fetal bovine serum (FBS, GIBCO, Invitrogen Co., Carlsbad, CA, USA), 50 U/ml penicillin, and 50 μg/ml streptomycin (Wako Pure Chemical Industries, Osaka, Japan).

2.2. Generation of mouse bone marrow-derived DCs

DCs were generated from bone marrow cells, as described elsewhere [30]. Briefly, bone marrow cells were isolated from C57BL/6 mice and were cultured in RPMI 1640 supplemented with 10% FBS, 50 μM 2-mercaptoethanol (Sigma Co., St. Louis, MO, USA), 50 U/ml penicillin, 50 μg/ml streptomycin, and 40 ng/ml mouse granulocyte-macrophage colony-stimulating factor (GM-CSF, PeproTech Inc., Rocky Hill, NJ, USA). After 8–16 days of culture, non-adherent cells were collected and used as DCs.

2.3. Preparation of BLs

Liposomes composed of 1,2-distearoyl-sn-glycero-phosphatidylcholine (DSPC) (NOF Co., Tokyo, Japan) and 1,2-distearoyl-sn-glycero-3-phosphatidyl-ethanolamine-methoxypolyethyleneglycol (DSPE-PEG (2 k)-OMe (NOF Co.)), 94:6 (mol:mol), were prepared by reverse phase evaporation. BLs were prepared from the liposomes and perfluoropropane (Takachiho Chemical Industrial Co., Ltd., Tokyo, Japan) as reported before [31,32]. Briefly, 5-ml sterilized vials containing 2 ml of the liposome suspension (lipid concentration: 2 mg/ml) were filled with perfluoropropane, capped, and then supercharged with 7.5 ml of perfluoropropane. The vials were placed in a bath-type sonicator (42 kHz, 100 W; BRANSONIC 2510J-DTH, Branson Ultrasonics Co., Danbury, CT, USA) for 5 min to form the BLs. In this method, the liposomes were reconstituted by sonication under the condition of supercharge with perfluoropropane in the 5-ml vial container. At the same time, perfluoropropane would be entrapped within lipids as micelles (composed of DSPC and DSPE-PEG(2k)-OMe), so forming nanobubbles. The lipid nanobubbles were encapsulated within the reconstituted liposomes, the sizes of which were increased from ~150–200 nm to ~500 nm.

2.4. Extraction of antigens from B16/BL6 cells

The extraction of antigens from B16BL/6 cells was performed by a butanol extraction method [33]. B16/BL6 cells were washed twice with phosphate-buffered saline (PBS) and then incubated with PBS containing 2.5% (v/v) 1-butanol. The solution was collected and centrifuged twice at 1600 ×*g* at 4 °C. The supernatant was dialyzed with water using a Spectra/Por Dialysis Membrane (MWCO: 10,000; Spectrum Laboratories, Inc., Rancho Dominguez, CA, USA). The dialysate then was centrifuged at 1600 ×*g* at 4 °C, and the resulting supernatant was freeze-dried.

2.5. FITC-dextran or B16/BL6-extracted antigen delivery following inhibition of the endocytic pathway in DCs

B16/BL6-extracted antigens were labeled with Alexa Fluor 633 Succinimidyl Esters (Invitrogen Co., Carlsbad, CA, USA) (Alexa-B16/BL6). DCs were pretreated with OptiMEM (Invitrogen Co.) containing 10 mM NaN_3 for 1 h at 4 °C to inhibit the endocytic pathway [34,35]. After washing the cells, BLs (120 μg) and FITC-dextran (Sigma Co.) or Alexa-B16/BL6 were added to the DCs in OptiMEM containing 10 mM NaN_3. The DCs were exposed to ultrasound (frequency: 2 MHz, duty: 10%, burst rate: 2.0 Hz, intensity 2.0 W/cm^2, time: 3 × 10 s (interval: 10 s)) using a Sonopore 4000 (6-mm diameter probe; Nepa Gene Co. Ltd., Chiba, Japan), then washed with PBS containing 10 mM NaN_3. The delivery efficiency of FITC-dextran or Alexa-B16/BL6 delivery was analyzed by flow cytometry [36].

2.6. Immunization with antigen-loaded DCs following BLs and ultrasound

DCs (2.5×10^5 cells) were pulsed with antigens (50 μg) exposed to ultrasound and/or BLs (120 μg) in a 48-well plate; the contents of 10 wells then were collected, pooled, and seeded into 1 well of a 6-well plate. After 1 h of incubation at 37 °C, the DCs were washed with medium and cultured for 24 h at 37 °C. The cells were washed with PBS, and the DCs (1×10^6 cells/100 μl) then were injected intradermally into the backs of C57BL/6 mice twice with a one-week interval.

2.7. B16/BL6 experimental lung metastasis model

C57BL/6 mice were immunized twice with DCs as described above. Seven days after the second immunization, B16/BL6 cells (1×10^5 cells/100 μl) were injected into the tail vein. The mice were sacrificed two weeks after the tumor cell injection, and the lungs were harvested and fixed in neutral buffered formalin (10%). The number of B16/BL6 colonies present on the surface of each set of lungs was determined by visual inspection using a stereoscopic dissecting microscope [37].

2.8. Statistical analysis

Differences in the number of lung metastatic colonies between the experimental groups were compared using non-repeated measures analysis of variance (ANOVA) with post-hoc Dunnett's test.

3. Results

3.1. FITC-dextran delivery into DCs by BLs and ultrasound

In BL/ultrasound antigen delivery, extracellular antigens are delivered into cells via the formation of transient membrane pores. Therefore, this technique is expected to deliver antigens into DCs as a function of both

pore size and molecular substrate size. In the present study, we used various molecular weight (MW) FITC-dextran molecules as model antigens and assessed the delivery efficiency of FITC-dextran into DCs. (Fig. 1(a–c)). In DCs treated with FITC-dextran (MW 4000) alone, the mean fluorescence intensity was 4-fold higher than non-treated DCs (Fig. 1(a)). On the other hand, upon treatment with FITC-dextran, BLs, and ultrasound, the mean fluorescence intensity was 2-fold higher than that with FITC-dextran alone. We also observed similar phenomena upon treatment with other sizes of FITC-dextran (MW 20,000 and 70,000) (Fig. 1(b), (c)). In addition, to assess the effect of molecular size on delivery efficiency, the fluorescence intensity was compared among FITC-dextrans (MW 4000, 20,000 and 70,000) delivered with BLs and ultrasound (Fig. 1(d)). The percentages of FITC-positive cells (M1 gated) were not affected by molecular weight, determined as 86.0% (MW: 4000), 87.3% (MW: 20,000), and 77.4% (MW: 70,000). On the other hand, the fluorescence intensity decreased as the molecular weight increased. The mean of fluorescence intensities were 24.5 (MW: 4000), 22.4 (MW: 20,000), and 16.5 (MW: 70,000).

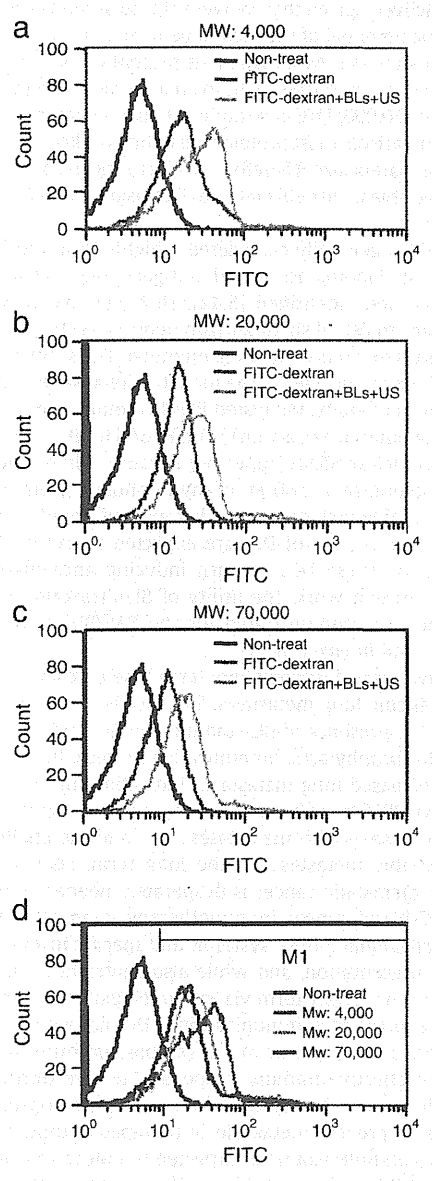

Fig. 1. Effect of molecular size on delivery into DCs using BLs and ultrasound. DCs were incubated with FITC-dextran, exposed to ultrasound in the presence of BLs, and washed with PBS. Delivery efficiency of FITC-dextran was analyzed using flow cytometry. Endocytosis by the DCs was inhibited by the inclusion of 10 mM sodium azide in all solutions and washes. Panels (a) to (c): Experiments were performed with FITC-dextran at a molecular weight of 4000, 20,000, or 70,000, respectively. Panel (d): Molecular weight dependency was analyzed following treatment with the combination of BLs and ultrasound. The percentages of M1 gated cell were quantified as follow: MW: 4000: 86.0%, MW: 20,000: 87.3%, MW: 70,000: 77.4%. The mean of fluorescent intensities were quantified as follow: MW: 4000: 24.5, MW: 20,000: 22.4, MW: 70,000: 16.5.

3.2. B16/BL6-extracted antigen delivery into DCs by BLs and ultrasound

Having demonstrated that the combination of BLs and ultrasound could deliver extracellular molecules of varying sizes, we sought to demonstrate that antigens extracted from B16/BL6 cells could be delivered into DCs by the same technique. Therefore, we assessed the delivery efficiency using Alexa Fluor 633-labeled antigens derived from B16/BL6 cells (Alexa-B16/BL6). As shown in Fig. 2, the DCs treated with antigens or the DCs treated with antigens and either BLs or ultrasound had fluorescence intensity profiles similar to those of untreated DCs. Flow cytometry confirmed this resemblance, with the percentages of Alexa-B16/BL6-positive cells (M2 gated) determined as 5.7% (antigen only), 6.5% (antigen and BLs), and 7.3% (antigen and ultrasound). In contrast, DCs treated with the combination of all three factors (antigens, BLs, and ultrasound) had an elevated fluorescence intensity profile compared with the other groups. Flow cytometry revealed that the percentage of Alexa-B16/BL6-positive cells was 74.1%.

3.3. Reduction in B16/BL6 lung metastasis following immunization with treated DCs

We employed an *in vivo* B16/BL6 experimental lung metastasis model to determine the anti-metastasis efficacy of DCs treated with tumor antigens delivered using BLs and ultrasound. C57BL/6 mice were immunized twice with bone marrow-derived DCs that were either untreated (no antigen exposure) or into which antigens had been delivered by one of four regimens (antigen alone; antigen + BLs; antigen + ultrasound; or antigen + BLs + ultrasound). As shown in Fig. 3(a), immunization with DCs that had been exposed to no antigen, antigen alone, or antigen with BLs *or* ultrasound weakly suppressed tumor metastasis. In contrast, immunization with DCs that had been exposed to antigens delivered via BLs *and* ultrasound reduced lung metastases four-fold, a decrease that was statistically significant ($P<0.05$) compared to the other groups. These numbers were consistent with the results of macroscopic inspection of lungs from the mice by stereoscopic microscopy, as shown in Fig. 3(b).

4. Discussion

The combination of ultrasound and microbubbles/nanobubbles has been reported to be an effective non-viral gene delivery method

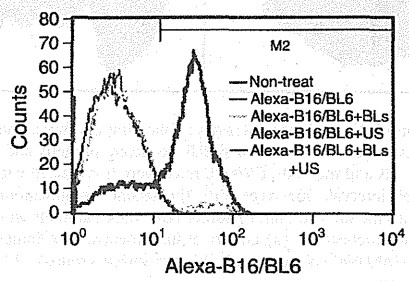

Fig. 2. Intracellular Alexa-B16/BL6 delivery into DCs using BLs and ultrasound. DCs were incubated with Alexa-labeled B16/BL6 extract, exposed (as indicated) to ultrasound and/or BLs, and washed with PBS. Delivery efficiency of Alexa-B16/BL6 was analyzed using flow cytometry. Endocytosis by the DCs was inhibited by the inclusion of 10 mM sodium azide in all solutions and washes. The percentages of M2 gated cell were quantified as follows: Alexa-B16/BL6: 5.7%; Alexa-B16/BL6 + BLs: 6.5%; Alexa-B16/BL6 + ultrasound 7.3%; Alexa-B16/BL6 + BLs + ultrasound: 74.1%.

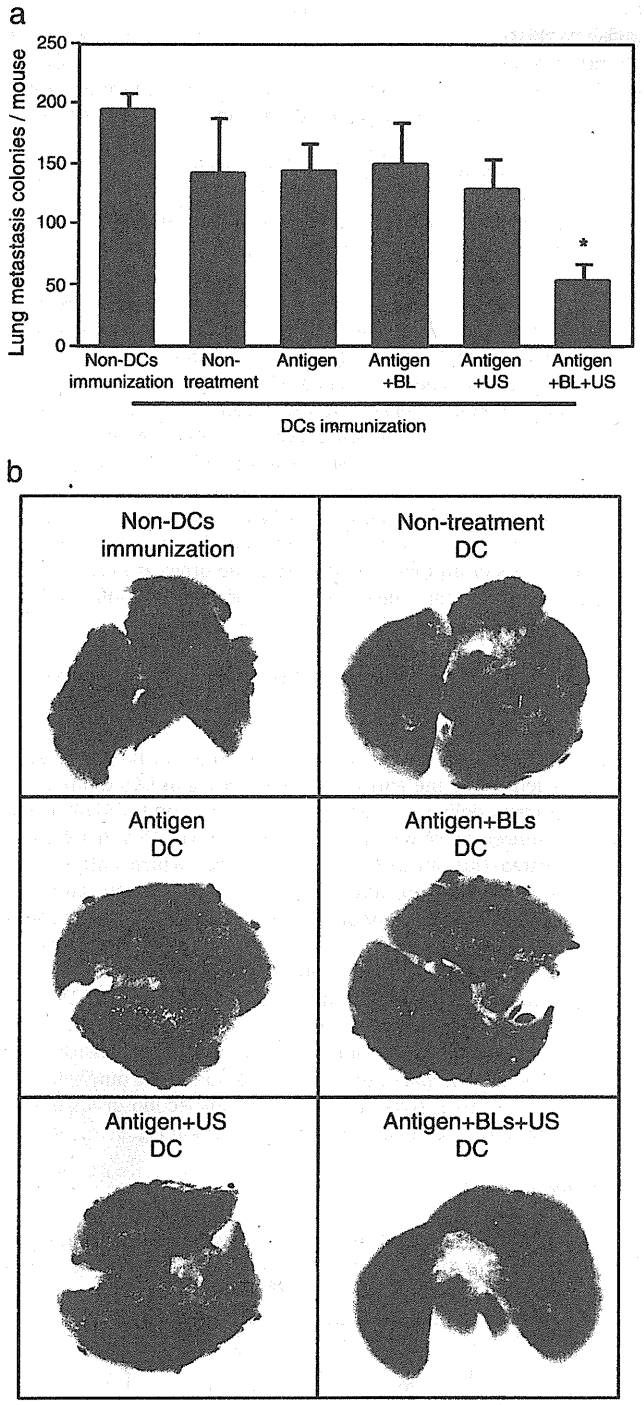

Fig. 3. Reduction of B16/BL6 lung metastasis following immunization with B16/BL6-treated DCs. DCs were treated with B16/BL6-extracted antigens and cultured as described in Materials and methods. C57BL/6 mice were immunized with the DCs twice with a one-week interval. One week after the second immunization, B16/BL6 cells were injected into the tail vein; after another two weeks, animals were sacrificed and lungs assessed for metastases. (a) Counts of lung metastatic colonies (means ± SDs; $n = 6$). *$P < 0.05$ (ANOVA, comparing all DC-immunized groups). (b) Images of lung by stereomicroscope.

for whole cells. This technique also has been applied for peptide and protein delivery [38–40]. In a previous study, we proposed the use of this technique for the delivery of novel antigens into DCs for cancer immunotherapy [29]. Entry into cells is believed to reflect the presence of transient pores in the cell membrane, permitting extracellular molecules direct access to the cytosol [21,28,41]. The present study confirmed that antigen was delivered into DCs by the combination of BLs and ultrasound, with delivery observed despite inhibition of the endocytic pathway. Thus, BLs appear to play a role similar to that of microbubbles for ultrasound-mediated substrate delivery. The present study also demonstrated an inverse correlation between the size of the substrate (MW of FITC-dextran) and the efficiency of delivery (fluorescence intensity). These results are consistent with a dependence of antigen delivery on pore size, which in turn depends on the degree of sonoporated cell membranes by BLs. The effect of pore size is expected to limit the delivery of larger molecules. However, this effect should not prevent the application of BL/ultrasound methods for antigen delivery, given that we were able to demonstrate the immunotherapeutic potential of the technique in an *in vivo* mouse model of lung cancer metastasis. As shown in the present work, we still observed delivery (albeit at a reduced level) even for a molecule (FITC-dextran) with a MW of 70,000. FITC-dextran is a bulky polymer with a straight chain; by comparison, most proteins are tightly packed, with a resulting decrease in apparent size. Therefore, various antigens of a range of sizes should still be able to be delivered into DCs using the BL/ultrasound delivery system.

Melanoma is generally considered a highly immunogenic cancer, and several melanoma-associated antigens (e.g., MAGE, MART-1, gp-100) have been identified [8,42]. However, we thought that it was important to establish an antigen delivery system that was suitable for various extracts containing unknown TAAs, since such a technique would be applicable for the induction of a variety of CTL clones [6]. In the present study, we tested BL/ultrasound delivery with TAAs obtained (via butanol extraction) from B16/BL6 cells. The use of butanol extraction is especially appealing because this method has been shown to solubilize a subset of hydrophobic proteins [33] that would presumably include various known and novel TAAs. Antigens delivered to the cytosol of DCs are expected to induce MHC class I presentation by these DCs, in turn inducing antigen-specific CTLs [12]. In the present work, the utility of BL/ultrasound delivery of a crude extract was demonstrated for the B16/BL6 antigens both *in vitro* (Fig. 2) and *in vivo* (Fig. 3).

The *in vivo* assay described here tested the efficacy of B16/BL6 antigens in reducing lung metastasis. Specifically, DCs were exposed to antigens in the presence of BLs and ultrasound, and the treated cells were used for prophylactic immunization of mice. Immunization significantly decreased lung metastasis, indicating that the treated DCs induced a B16/BL6-specific anti-tumor immune response. Given the poor prognosis seen with metastases [3,4], and the challenge of preventing systemic metastasis in the long term, such a therapeutic strategy for metastatic cancer is desperately needed. From this perspective, DC-based cancer immunotherapy is an attractive option: this approach should induce systemic and specific immune responses via antigen presentation, and while also controlling metastasis and recurrence in the longer term via immunological memory [6]. Matheoud et al. reported that immunization of DCs has a potency to reduce the metastasis in therapeutic model (by post-immunization) [43]. To induce more effective immune responses, we are optimizing about antigen delivery for DCs by BLs/ultrasound. After optimization, we will attempt to prevent metastasis in therapeutic model. The combination of BLs and ultrasound is expected to induce effective immune response in DC-based cancer immunotherapy by delivering various TAAs into DCs for potential clinical applications.

Acknowledgments

The authors thank Mr. Eisuke Namai, Mr. Yasuyuki Shiono, Mr. Ken Osawa, Ms. Motoka Kawamura, Mr. Ryo Tanakadate, Mr. Kunihiko Matsuo, Mr. Yudai Kawashima, Mr. Hitoshi Uruga, and Ms. Mutsumi Seki (Teikyo University) for their technical assistance,

and Mr. Yasuhiko Hayakawa and Mr. Kosho Suzuki (Nepa Gene Co., Ltd.) for their technical advice regarding ultrasound exposure. This study was supported by the Program for Promotion of Fundamental Studies in Health Sciences of the National Institute of Biomedical Innovation (NIBIO). This work was supported by JSPS KAKENHI (20240053 and 23300192) and Health and Labour Science Research Grants from Ministry of Health, Labour and Welfare.

References

[1] J.W. Gamel, S.L. George, M.J. Edwards, H.F. Seigler, The long-term clinical course of patients with cutaneous melanoma, Cancer 95 (2002) 1286–1293.
[2] C.M. Balch, S.J. Soong, M.B. Atkins, A.C. Buzaid, A. Houghton Jr., J.M. Kirkwood, K.M. McMasters, M.F. Mihm, D.L. Morton, D.S. Reintgen, M.I. Ross, A. Sober, J.A. Thompson, J.F. Thompson, An evidence-based staging system for cutaneous melanoma, CA Cancer J. Clin. 54 (2004) 131–149.
[3] C. Garbe, P. Terheyden, U. Keiholz, O. Kolbl, A. Hauschild, Treatment of melanoma, Dtsch. Arztebl. Int. 105 (2008) 845–851.
[4] U. Vaishampayan, J. Abrams, D. Darrah, V. Joñes, M.S. Mitchell, Active immunotherapy of metastatic melanoma with allogeneic melanoma lysates and interferon, Clin. Cancer Res. 3696 (2002) 3696–3701.
[5] E.M. Levy, M.P. Roberti, J. Mordoh, Natural kiiller cells in human cancer: from biological functions to clinical applications, J. Biomed. Biotechnol. 2011 (2011) 676198.
[6] K. Palucka, H. Ueno, J. Banchereau, Recent developments in cancer vaccines, J. Immunol. 186 (2011) 1325–1331.
[7] P.W. Kantoff, C.S. Higano, N.D. Shore, E.R. Berger, E.J. Small, D.F. Penson, C.H. Redfern, A.C. Ferrari, R. Dreicer, R.B. Sims, Y. Xu, M.W. Frohlich, P.F. Schellhammer, Sipuleucel-T immunotherapy for castration-resistant prostate cancer, N. Engl. J. Med. 363 (2010) 411–422.
[8] S.A. Rosenberg, J.C. Yang, P.F. Robbins, J.R. Wunderlich, P. Hwu, R.M. Sherry, D.J. Schwartzentruber, S.L. Topalian, N.P. Restifo, A. Filie, R. Chang, M.E. Dudley, Cell transfer therapy for cancer: lessons from sequential treatment of a patient with metastatic melanoma, J. Immunother. 26 (2003) 385–393.
[9] P.W. Kantoff, T.J. Schuetz, B.A. Blumenstein, L.M. Glode, D.L. Bilhartz, M. Wyand, K. Manson, D.L. Panicali, R. Laus, J. Schlom, W.L. Dahut, P.M. Arlen, J.L. Gulley, W.R. Godfrey, Overall survival analysis of a phase II randomized controlled trial of a poxviral based PSA-targeted immunotherapy in metastatic castration-resistant prostate cancer, J. Clin. Oncol. 28 (2010) 1099–1105.
[10] F.O. Nestle, A. Farkas, C. Conrad, Dendritic-cell-based therapeutic vaccination against cancer, Curr. Opin. Immunol. 17 (2005) 163–169.
[11] J. Copier, A. Dalgleish, Overview of tumor cell-based vaccines, Int. Rev. Immunol. 25 (2006) 297–319.
[12] R.N. Germain, MHC-dependent antigen processing and peptide presentation: providing ligands for T lymphocyte activation, Cell 76 (1994) 287–299.
[13] P.A. Antony, C.A. Piccirillo, A. Akpinarli, S.E. Finkelstein, P.J. Speiss, D.R. Surman, D.C. Palmer, C.C. Chan, C.A. Klebanoff, W.W. Overwijk, S.A. Rosenberg, N.P. Restifo, CD8+ T cell immunity against a tumor/self-antigen is augmented by CD4+ T helper cells and hindered by naturally occurring T regulatory cells, J. Immunol. 174 (2005) 2591–2601.
[14] P. Elamanchili, M. Diwan, M. Cao, J. Samuel, Characterization of poly(D, L-lactic-co-glycolic acid) based nanoparticulate system for enhanced delivery of antigens to dendritic cells, Vaccine 22 (2004) 2406–2412.
[15] N. Okada, T. Saito, K. Mori, Y. Masunaga, Y. Fujii, J. Fujita, K. Fujimoto, T. Nakanishi, K. Tanaka, S. Nakagawa, T. Mayumi, T. Fujita, A. Yamamoto, Effects of lipofectin-antigen complexes on major histocompatibility complex class I-restricted antigen presentation pathway in murine dendritic cells and on dendritic cell maturation, Biochem. Biophys. Acta 1527 (2001) 97–101.
[16] K. Kawamura, N. Kadowaki, R. Suzuki, S. Udagawa, S. Kasaoka, N. Utoguchi, T. Kitawaki, N. Sugimoto, N. Okada, K. Maruyama, T. Uchiyama, Dendritic cells that endocytosed antigen-containing IgG-liposomes elicit effective antitumor immunity, J. Immunother. 29 (2006) 165–174.
[17] T. Yoshikawa, N. Okada, A. Oda, K. Matsuo, K. Matsuo, Y. Mukai, Y. Yoshioka, T. Akagi, M. Akashi, S. Nakagawa, Development of amphiphilic gamma-PGA-nanoparticle based tumor vaccine: potential of the nanoparticulate cytosolic protein delivery carrier, Biochem. Biophys. Res. Commun. 366 (2008) 408–413.
[18] L. Wang, H. Ikeda, Y. Ikuta, M. Schmitt, Y. Miyahara, Y. Takahashi, X. Gu, Y. Nagata, Y. Sasaki, K. Akiyoshi, J. Sunamoto, H. Nakamura, K. Kuribayashi, H. Shiku, Bone marrow-derived dendritic cells incorporate and process hydrophobized poly-saccaride/oncoprotein complex as antigen presenting cells, Int. J. Oncol. 14 (1999) 695–701.
[19] P. Machy, K. Serre, L. Leserman, Class I-restricted presentation of exogenous antigen acquired by Fcgammareceptor-mediated endocytosis is regulated in dendritic cells, Eur. J. Immunol. 30 (2000) 848–857.
[20] W.J. Greenleaf, M.E. Bolander, G. Sarkar, M.B. Goldring, J.F. Greenleaf, Artificial cavitation nuclei significantly enhance acoustically induced cell transfection, Ultrasound Med. Biol. 24 (1998) 587–595.
[21] Y. Taniyama, K. Tachibana, K. Hiraoka, M. Aoki, S. Yamamoto, K. Matsumoto, T. Nakamura, T. Ogihara, Y. Kaneda, R. Morishita, Development of safe and efficient novel nonviral gene transfer using ultrasound: enhancement of transfection efficiency of naked plasmid DNA in skeletal muscle, Gene Ther. 9 (2002) 372–380.
[22] S. Chen, J.H. Ding, R. Bekeredjian, B.Z. Yang, R.V. Shohet, S.A. Johnston, H.E. Hohmeier, C.B. Newgard, P.A. Grayburn, Efficient gene delivery to pancreatic islets with ultrasonic microbubble destruction technology, Proc. Natl. Acad. Sci. U. S. A. 103 (2006) 8469–8474.
[23] A. Aoi, Y. Watanabe, S. Mori, M. Takahashi, G. Vassaux, T. Kodama, Herpes simplex virus thymidine kinase-mediated suicide gene therapy using nano/microbubbles and ultrasound, Ultrasound Med. Biol. 34 (2008) 425–434.
[24] Z.P. Shen, A.A. Brayman, L. Chen, C.H. Miao, Ultrasound with microbubbles enhances gene expression of plasmid DNA in the liver via intraportal delivery, Gene Ther. 15 (2008) 1147–1155.
[25] S. Sonoda, K. Tachibana, E. Uchino, A. Okubo, M. Yamamoto, K. Sakoda, T. Hisatomi, K.H. Sonoda, Y. Negishi, Y. Izumi, S. Takao, T. Sakamoto, Gene transfer to corneal epithelium and keratocytes mediated by ultrasound with microbubbles, Investig. Ophthalmol. Vis. Sci. 47 (2006) 558–564.
[26] K. Iwanaga, K. Tominaga, K. Yamamoto, M. Habu, H. Maeda, S. Akifusa, T. Tsujisawa, T. Okinaga, J. Fukuda, T. Nishihara, Local delivery system of cytotoxic agents to tumors by focused sonoporation, Cancer Gene Ther. 14 (2007) 354–363.
[27] Y. Taniyama, K. Tachibana, K. Hiraoka, T. Namba, K. Yamasaki, N. Hashiya, M. Aoki, T. Ogihara, K. Yasufumi, R. Morishita, Local delivery of plasmid DNA into rat carotid artery using ultrasound, Circulation 105 (2002) 1233–1239.
[28] R. Suzuki, Y. Oda, N. Utoguchi, K. Maruyama, Progress in the development of ultrasound-mediated gene delivery systems utilizing nano- and microbubbles, J. Control. Release 149 (2011) 36–41.
[29] R. Suzuki, Y. Oda, N. Utoguchi, E. Namai, Y. Taira, N. Okada, N. Kadowaki, T. Kodama, K. Tachibana, K. Maruyama, A novel strategy utilizing ultrasound for antigen delivery in dendritic cell-based cancer immunotherapy, J. Control. Release 133 (2009) 198–205.
[30] K. Inaba, M. Inaba, M. Deguchi, K. Hagi, R. Yasumitsu, S. Ikehara, S. Muramatsu, R.M. Steinman, Granulocytes, macrophages, and dendritic cells arise from a common major histocompatibility complex class II-negative progenitor in mouse bone marrow, Proc. Natl. Acad. Sci. U. S. A. 90 (1993) 3038–3042.
[31] R. Suzuki, T. Takizawa, Y. Negishi, K. Hagisawa, K. Tanaka, K. Tanaka, K. Sawamura, N. Utoguchi, T. Nishioka, K. Maruyama, Gene delivery by the combination of novel liposomal bubbles with perfluoropropane and ultrasound, J. Control. Release 117 (2007) 130–136.
[32] R. Suzuki, T. Takizawa, Y. Negishi, N. Utoguchi, K. Sawamura, K. Tanaka, E. Namai, Y. Oda, Y. Matsumura, K. Maruyama, Tumor specific ultrasound enhanced gene transfer in vivo with novel liposomal bubbles, J. Control. Release 125 (2008) 137–144.
[33] N. Labateya, D.M.P. Thomson, M. Durko, G. Shenouda, L. Robb, R. Scanzano, Extraction of human organ-specific cancer neoantigens from cancer cell and plasma membranes with 1-butanol, Cancer Res. 47 (1987) 1058–1064.
[34] I.A. Ignatovich, E.B. Dizhe, A.V. Pavlotskaya, B.N. Akifiev, S.V. Burov, S.V. Orlov, A.P. Perevozchikov, Complexes of plasmid DNA with basic domain 47–57 of the HIV-1 Tat protein are transferred to mammalian cells by endocytosis-mediated pathways, J. Biol. Chem. 278 (2003) 42625–42636.
[35] K. Sandvig, S. Olsnes, Entry of the toxic proteins abrin, modeccin, ricin, and diphtheria toxin into cells. II. Effect of pH, metabolic inhibitors, and ionophores and evidence for toxin penetration from endocytotic vesicles, J. Biol. Chem. 257 (1982) 7504–7513.
[36] D.A. Zaharoff, J.W. Henshaw, B. Mossop, F. Yuan, Mechanistic analysis of electroporation-induced cellular uptake of macromolecules, Exp. Biol. Med. 233 (2008) 94–105.
[37] J.G. Naglich, M. Jure-Kunkel, E. Gupta, J. Fargnoli, A.J. Henderson, A.C. Lewin, R. Talbott, A. Baxter, J. Bird, R. Savopoulos, R. Wills, R.A. Kramer, P.A. Trail, Inhibition of angiogenesis and metastasis in two murine models by the matrix metalloproteinase inhibitor, BMS-275291, Cancer Res. 61 (2001) 8480–8485.
[38] R. Bekeredjian, S. Chen, P.A. Grayburn, R.V. Shohet, Augmentation of cardiac protein delivery using ultrasound targeted microbubble destruction, Ultrasound Med. Biol. 31 (2005) 687–691.
[39] R. Bekeredjian, H.F. Kuecherer, R.D. Kroll, H.A. Katus, S.E. Hardt, Ultrasound-targeted microbubble destruction augments protein delivery in testes, Urology 69 (2007) 386–389.
[40] M. Kinoshita, K. Hynynen, Intracellular delivery of Bak BH3 peptide by microbubble-enhanced ultrasound, Pharm. Res. 22 (2005) 149–156.
[41] M. Duvshani-Eshet, D. Adam, M. Machluf, The effect of albmin-coated microbubbles in DNA delivery mediated by therapeutic ultrasound, J. Control. Release 112 (2005) 156–166.
[42] P. van der Bruggen, C. Traversari, P. Chomez, C. Lurguin, E. De Plaen, B. Van den Eynde, A. Knuth, T. Boon, A gene encoding an antigen recognized by cytolytic T lymphocytes on a human melanoma, Science 254 (1991) 1643–1647.
[43] D. Matheoud, C. Baey, L. Vimeux, A. Tempez, M. Valente, P. Louche, A.L. Bon, A. Hosmalin, V. Feuillet, Dendritic cells crosspresent antigens from live B16 cells more efficiently than from apoptotic cells and protect from melanoma in a therapeutic model, PLoS One 6 (4) (2011) e19104.

International Journal of Pharmaceutics 422 (2012) 504–509

Contents lists available at SciVerse ScienceDirect

International Journal of Pharmaceutics

journal homepage: www.elsevier.com/locate/ijpharm

Pharmaceutical nanotechnology

Efficient siRNA delivery using novel siRNA-loaded Bubble liposomes and ultrasound

Yoko Endo-Takahashi[a,1], Yoichi Negishi[a,*,1], Yasuharu Kato[a], Ryo Suzuki[b], Kazuo Maruyama[b], Yukihiko Aramaki[a]

[a] Department of Drug Delivery and Biopharmaceutics, School of Pharmacy, Tokyo University of Pharmacy and Life Sciences, Hachioji, Tokyo, Japan
[b] Department of Biopharmaceutics, School of Pharmaceutical Sciences, Teikyo University, Sagamihara, Kanagawa, Japan

ARTICLE INFO

Article history:
Received 8 July 2011
Received in revised form 18 October 2011
Accepted 13 November 2011
Available online 22 November 2011

Keywords:
siRNA delivery
Ultrasound
Bubble liposomes

ABSTRACT

Recently, we developed novel polyethyleneglycol (PEG)-modified liposomes (Bubble liposomes; BLs) entrapping an ultrasound (US) imaging gas and reported that the combination of BLs and US was useful for the delivery of siRNA directly into the cytoplasm. However, the results were obtained using a mixture of BLs and naked siRNA. With systemic injections, it is important to control the biodistribution of both BLs and siRNA. In addition, the delivery of siRNA is affected by nuclease degradation after intravenous administration. In this study, we prepared novel siRNA-loaded BLs (si-BLs) using a cationic lipid, 1,2-dioleoyl-3-trimethylammonium-propane (DOTAP). We demonstrated that siRNA could be loaded onto BLs containing DOTAP and that siRNA-loaded BLs were stable in serum. A specific gene-silencing effect was also achieved by transfection with si-BLs. Thus, the combination of si-BLs with US exposure can be used for delivery of siRNA to a specific tissue via systemic injection.

1. Introduction

RNA interference (RNAi) has potential application in the development of new therapies for malignant, infectious, and autoimmune diseases. Indeed, synthetic siRNAs are capable of knocking down targets *in vivo* (Frank-Kamenetsky et al., 2008; Halder et al., 2006; Kim et al., 2008; McCaffrey et al., 2002; Morrissey et al., 2005; Niu et al., 2006; Sato et al., 2008; Song et al., 2003; Takeshita et al., 2005; Xia et al., 2007). However, effective and nontoxic delivery is the major challenge to its implementation in a clinical setting.

One novel approach to the administration of a drug or gene is ultrasound (US)-enhanced delivery, which exploits cavitation bubbles produced by the pressure oscillations of US. US pressures above a certain threshold can cause oscillating bubbles to collapse violently, a process known as inertial cavitation. Inertial cavitation is believed to temporarily improve the permeability of cell membranes, enabling the transport of extracellular molecules into viable cells (Delius and Adams, 1999; Duvshani-Eshet and Machluf, 2005; Greenleaf et al., 1998; Holmes et al., 1992; Schratzberger et al., 2002). Furthermore, in combination with microbubbles, contrast agents for medical US imaging improve siRNA transfection efficiency (Du et al., 2011; Kinoshita and Hynynen, 2005; Otani et al., 2009; Tsunoda et al., 2005). However, microbubbles have problems with size, stability, and targeting functionality.

Polyethyleneglycol (PEG)-modified liposomes have excellent biocompatibility, stability, and a long circulation time and can be easily prepared in a variety of sizes and modified to add a targeting function. For these reasons, they are widely used as carriers of drugs, antigens, and genes (Allen et al., 1991; Blume and Cevc, 1990; Harata et al., 2004; Maruyama et al., 1992, 2004). Therefore, PEG-liposomes containing a US imaging gas could be used as novel gene delivery agents. We recently reported that "Bubble liposomes" (BLs) were suitable for gene delivery *in vitro* and *in vivo* (Negishi et al., 2011b,c; Suzuki et al., 2007, 2008a,b). Furthermore, we showed that the combination of BLs and US was also useful for the delivery of siRNA *in vitro* and *in vivo* and that siRNA was introduced directly into the cytoplasm (Negishi et al., 2008). However, the results were obtained using a mixture of BLs and naked siRNA. With systemic injections, transfection efficiency is reduced if the BLs and siRNA are not colocalized in blood vessels. Therefore, it is important to control the biodistribution of both BLs and siRNA. In addition, siRNA is degraded by nuclease and removed rapidly from the circulation after intravenous administration. To overcome these problems, the loading of siRNA onto BLs could be effective for siRNA delivery. Recently, it has been reported that PEGylated lipoplexes (PEG-siPlex) bound to microbubbles led to an increase in the local lipoplex concentration near the cell membrane and resulted in much higher transfection with siRNA in the presence of US (Lentacker et al., 2009; Vandenbroucke et al., 2008). It was also shown that the delivery of siRNA by siRNA-microbubble complexes

* Corresponding author. Tel.: +81 42 676 3183; fax: +81 42 676 3183.
E-mail address: negishi@toyaku.ac.jp (Y. Negishi).
[1] These authors contributed equally to this work.

0378-5173/$ – see front matter © 2011 Elsevier B.V. All rights reserved.
doi:10.1016/j.ijpharm.2011.11.023

was effective for transfection into arteries (Suzuki et al., 2010). However, microbubbles were used in these reports. Microbubbles have problems with size, stability, and targeting functionality as mentioned above. Therefore, we developed nanosized, siRNA-loaded BLs using cholesterol-conjugated siRNA (chol-si-BLs) and demonstrated that using chol-si-BLs led to the stability of siRNA (Negishi et al., 2011a). In this study, we prepared siRNA-loaded BLs (si-BLs) using a cationic lipid. Novel si-BLs were able easily prepared compared with chol-si-BLs. Additionally, this method may have widespread utility for drug delivery systems because it is applicable to various materials possessing negative electrical charges. We also investigated the effects of the amount of PEG in the BLs on their interaction with siRNA, the stability of siRNA in serum, and the gene-silencing effects of transfection with si-BLs and US.

2. Materials and methods

2.1. Cell lines and cultures

COS-7 cells were cultured in Dulbecco's modified Eagle's medium (DMEM; Kohjin Bio Co. Ltd., Tokyo, Japan) supplemented with 10% heat-inactivated fetal bovine serum (FBS; Equitech Bio Inc., Kerrville, TX), 100 units/mL penicillin, and 100 μg/mL streptomycin in a humidified atmosphere containing 5% CO_2 at 37 °C.

2.2. Preparation of liposomes and BLs

To prepare liposomes for conventional BLs, 1,2-dipalmitoyl-sn-glycero-phosphatidylcholine (DPPC) and 1,2-distearoylphosphatidylethanolamine-methoxy-polyethylene glycol (PEG_{2000}) were mixed at a molar ratio of 94:6. Both lipids were purchased from NOF Corporation (Tokyo, Japan). 1,2-dioleoyl-3-trimethylammonium-propane (DOTAP) and 1,2-distearoyl-sn-glycero-3-phosphoethanolamine-N-[methoxy(polyethylene glycol)-750] (PEG_{750}) from Avanti Polar Lipids (Alabaster, AL) were also used. Liposomes with various lipid compositions were prepared by a reverse-phase evaporation method, as described previously (Negishi et al., 2008). In brief, all reagents were dissolved in 1:1 (v/v) chloroform/diisopropylether. Phosphate-buffered saline was added to the lipid solution, and the mixture was sonicated and then evaporated at 47 °C. The organic solvent was completely removed, and the size of the liposomes was adjusted to less than 200 nm using extruding equipment and a sizing filter (Nuclepore Track-Etch Membrane, 200 nm pore size, Whatman plc, UK). After being sized, the liposomes were passed through a sterile 0.45-μm syringe filter (Asahi Techno Glass Co., Chiba, Japan) to sterilize them. The lipid concentration was measured using the Phospholipid C test (Wako Pure Chemical Industries, Ltd., Osaka, Japan). BLs were prepared from liposomes and perfluoropropane gas (Takachiho Chemical Inc., Co., Ltd., Tokyo, Japan). First, 5-mL sterilized vials containing 2 mL of liposome suspension (lipid concentration: 1 mg/mL) were filled with perfluoropropane gas, capped, and then pressurized with 7.5 mL of perfluoropropane gas. The vials were placed in a bath-type sonicator (42 kHz, 100 W, Bransonic 2510J-DTH, Branson Ultrasonics Co., Danbury, CT) for 5 min to form BLs. The zeta potential and mean size of the BLs were determined using the light-scattering method with a zeta potential/particle sizer (Nicomp 380ZLS, Santa Barbara, CA).

2.3. Ultrasound imaging of BLs

BLs diluted with PBS were dispensed into 6-well plates. B-mode recordings were made using a high-frequency ultrasound imaging system (NP60R-UBM, Nepa Gene, Co., Ltd., Chiba, Japan).

2.4. Plasmid DNA and siRNA

The plasmid pCMV-GL3, derived from pGL3-basic (Promega, Madison, WI), is an expression vector encoding the firefly luciferase gene under the control of a cytomegalovirus promoter. Small interfering RNA targeting luciferase (Luciferase GL3 siRNA; siGL3) and a nontargeting siRNA (Control (non-sil.) siRNA; siCont) were purchased from Qiagen K.K. (Tokyo, Japan). Their sequences were as follows: siGL3, *5′-CUUACGCUGAGUACUUCGAdTdT-3′* and *5′-UCGAAGUACUCAGCGUAAGdTdT-3′*; siCont, *5′-UUCUCCGAACGUGUCACGUdTdT-3′* and *5′-ACGUGACACGUUCGGAGAAdTdT-3′*. Nontargeting fluorescein-labeled siRNA (BLOCK-iT Fluorescent Oligo) was purchased from Invitrogen Japan K.K. (Tokyo, Japan).

2.5. Preparation of si-BLs

For the preparation of si-BLs, adequate amounts of siRNA were added to BLs and gently mixed. FITC-labeled siRNA and flow cytometry were used to examine the interaction between siRNA and BLs. The fluorescence intensity of si-BLs was analyzed using a FACSCanto (Becton Dickinson, San Jose, CA). To quantify the amount of siRNA loaded onto the BL surfaces, the BLs were centrifuged at 2000 rpm for 1 min and the unbound siRNA was removed. The BL solution and the aqueous solution containing the unbound siRNA were then boiled for 5 min after which the optical density was measured at 260 nm using a spectrophotometer.

2.6. Stability of siRNA in serum

The BLs, siRNA, and si-BLs were incubated in 50% serum for 15, 30, and 60 min. Serum was used without heat inactivation. The stability of the siRNA was confirmed by 15% polyacrylamide gel electrophoresis. The gel was stained with SYBR SAFE (Invitrogen Japan K.K., Tokyo, Japan) and visualized under ultraviolet light.

2.7. Transfection of siRNA into cells using BLs or si-BLs

The mixture of siRNA (final concentration 100 nM) and BLs or si-BLs (60 μg) in culture medium containing 10% FBS was added to the cells transfected with pDNA on the previous day. The cells were immediately exposed to US (frequency, 2 MHz; duty, 50%; burst rate, 2.0 Hz; intensity 2.0 W/cm^2) for 10 s through a 6-mm diameter probe placed in the well. A Sonopore 3000 (NEPA GENE, Co., Ltd., Chiba, Japan) was used to generate the US. The cells were washed twice with culture medium and cultured for two days.

To measure luciferase activity after transfection, cell lysate was prepared with a lysis buffer (0.1 M Tris–HCl (pH 7.8), 0.1% Triton X-100, and 2 mM EDTA). Luciferase activity was measured using a luciferase assay system (Promega, Madison, WI) and a luminometer (LB96 V, Belthold Japan Co., Ltd., Tokyo, Japan). The activity is reported in as relative light units (RLU) per mg of protein.

2.8. Statistical analyses

All data are reported as the mean ± SD ($n = 4$). Data were considered significant when $P < 0.05$. The t-test was used to calculate statistical significance.

3. Results

3.1. Preparation of BLs containing DOTAP

Initial experiments were performed to investigate whether liposomes containing a cationic lipid, DOTAP, could entrap a US imaging gas as well as conventional BLs. We prepared liposomes containing DOTAP in various amounts and attempted to entrap the gas. The

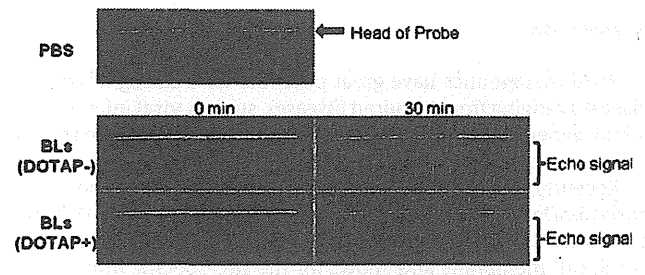

Fig. 1. Ultrasonographic images of a plate containing BLs with or without DOTAP.

liposomes containing up to 15 mol% DOTAP became cloudy, and we concluded that they could effectively entrap the imaging gas (data not shown). The liposomes containing more than 15 mol% DOTAP had difficulty entrapping the gas. We also examined BLs containing DOTAP using a high-frequency US imaging system. The system is a two-dimensional US image display composed of bright dots representing the US echoes. The brightness of each dot is determined by the amplitude of the returned echo signal. As shown in Fig. 1, the US echo signal was detected even 30 min later.

3.2. Effects of polyethyleneglycol on the interaction of siRNA with BLs

To assess whether siRNA could be loaded onto the surface of BLs, we used a fluorescence-activated cell sorter, the FACSCanto. We also prepared BLs containing different lengths of PEG to assess the effect of PEG on BL interactions with siRNA. As shown in Fig. 2, BLs not containing DOTAP were successfully loaded with siRNA. Approximately 40% of the BLs were FITC positive. Approximately 45% of the BLs containing DOTAP but not containing PEG_{750} were FITC positive. In contrast, BLs containing DOTAP and PEG_{750} were more heavily loaded with siRNA. Approximately 80% were FITC positive. Thus, in all subsequent experiments, BLs composed of DPPC, DOTAP, PEG_{2000}, and PEG_{750} (in a 79:15:3:3 molar ratio) were used.

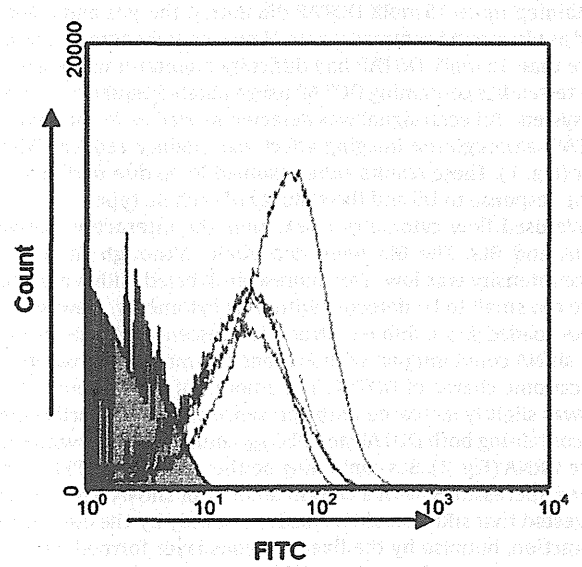

Fig. 2. Interaction of siRNA with BLs and the effects of PEG chain length on the interaction. The interaction was examined by analyzing a mixture of FITC-siRNA (50 pmol) and various BLs (60 μg) with the FACSCanto; gray area: BLs only; red curve: si-BLs (DOTAP (−), PEG_{2000} and PEG_{750} (molar ratio, 6:0)); green curve: si-BLs (DOTAP (+), PEG_{2000} and PEG_{750} (6:0)); blue curve: si-BLs (DOTAP (−), PEG_{2000} and PEG_{750} (3:3)); purple curve: si-BLs (DOTAP (+), PEG_{2000} and PEG_{750} (3:3)).

Table 1
Size (nm) and zeta potential (mV) of BLs and si-BLs.

Lipid composition of BLs (molar ratio)	BLs	si-BLs
DPPC:PEG_{2000} = 94:6	528.3 nm	587.9 nm
DPPC:DOTAP:PEG_{2000}:PEG_{750} = 79:15:3:3	749.0 nm	862.2 nm
DPPC:PEG_{2000} = 94:6	−0.81 mV	−0.42 mV
DPPC:DOTAP:PEG_{2000}:PEG_{750} = 79:15:3:3	−0.20 mV	−0.13 mV

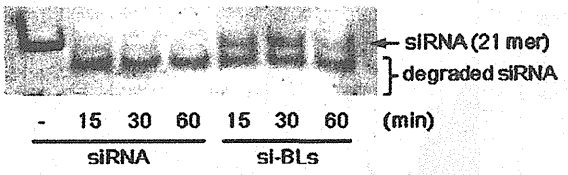

Fig. 3. Stability of siRNA in the presence of serum. Naked siRNA or si-BLs (DOTAP (+), PEG_{2000} and PEG_{750} (3:3)) were subjected to 50% serum degradation at 37 °C for 0.5 or 1 h and confirmed by 15% acrylamide gel electrophoresis.

As shown in Table 1, there was almost no change in the size and zeta potential of the BLs after siRNA was added.

We investigated the stability of siRNA in serum. Small interfering RNA held by BLs showed increased stability in 50% serum compared with free siRNA, although some siRNA was degraded (Fig. 3). We also examined the change in the amount of siRNA bound to BLs when the concentration of the siRNA was increased. As shown in Fig. 4, the amount siRNA loaded increased in a dose-dependent manner. We finally estimated that 60 μg of BLs could be loaded with at least 100 pmol of siRNA and that approximately 30% of the siRNA was bound to the lipid surface.

3.3. Transfection of siRNA into cells using BLs or si-BLs

Before the transfection experiments, we investigated the destruction efficiency of si-BLs under the US exposure. The solution of si-BLs was exposed to the same conditions used for *in vitro* transfection and was analyzed using the FACSCanto. Unlike the solution of si-BLs before US exposure, no fluorescence was detected in the

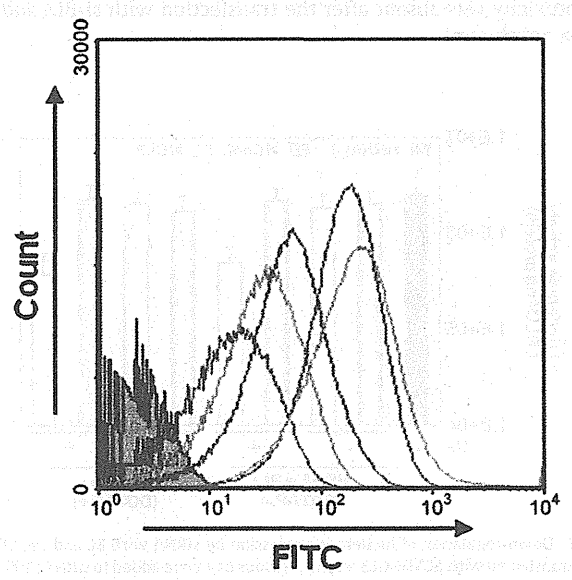

Fig. 4. Loading of siRNA onto BLs. The interaction was examined by analyzing a mixture of FITC-siRNA (12.5–200 pmol) and BLs (60 μg) containing DPPC, DOTAP, PEG_{2000} and PEG_{750} (79:15:3:3) with FACSCanto; gray area: BLs only; red curve: si-BLs (siRNA 12.5 pmol); green curve: si-BLs (siRNA 25 pmol); blue curve: si-BLs (siRNA 50 pmol); purple curve: s si-BLs (siRNA 100 pmol); light blue curve: si-BLs (siRNA 200 pmol).

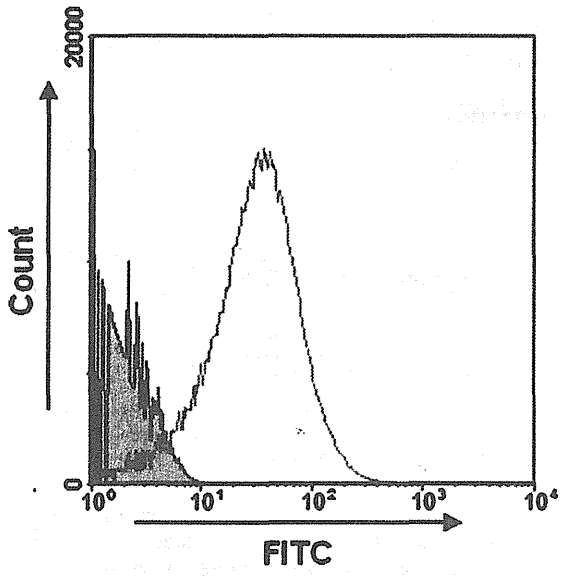

Fig. 5. Effects of US on si-BLs. The interaction was examined by analyzing a mixture of FITC-siRNA (50 pmol) and BLs (60 μg) containing DPPC, DOTAP, PEG_{2000}, and PEG_{750} (79:15:3:3) with the FACSCanto; gray area: BLs only; red curve: si-BLs; green curve: solution of si-BLs after US exposure (frequency, 2 MHz; duty, 50%; burst rate, 2.0 Hz; intensity, 2.0 W/cm^2; time, 10 s). (For interpretation of the references to color in this figure legend, the reader is referred to the web version of the article.)

solution (Fig. 5). This result suggested that the US caused the release of siRNA from the surface of the BLs.

To investigate the gene-silencing effects of siRNA transfection with si-BLs and US, cells transfected with pDNA encoding firefly luciferase (pCMV-GL3) on the previous day were added to BLs loaded with nontargeting control or luciferase-targeting siRNA (siCont or siGL3) and exposed to US (Fig. 6). Approximately 80% of luciferase expression was specifically blocked by siGL3 in the si-BLs-treated group and in the group treated with conventional BLs. Cytotoxicity was absent after the transfection with si-BLs and US (data not shown).

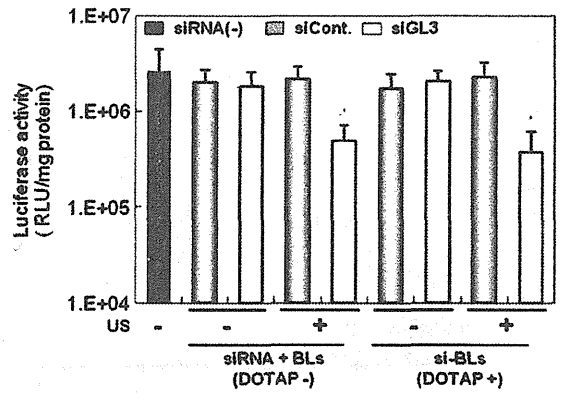

Fig. 6. Down-regulation of luciferase expression by siRNA with BL and US. COS-7 cells transfected with pCMV-GL3 on the previous day were added to siRNA (100 nM) and conventional BLs (DOTAP (−), PEG_{2000}, and PEG_{750} (molar ratio, 6:0)) or si-BLs (DOTAP (+), PEG_{2000}, and PEG_{750} (molar ratio, 3:3)) and applied. At 2 days posttransfection, luciferase expression was measured. siRNA(−); the group not transfected with siRNA, siCont; the group transfected with nontargeting siRNA (siCont), siGL3; the group transfected with siRNA targeting luciferase (siGL3). *P values <0.05 compared with the group transfected with siCont. All data are reported as the mean ± SD (n = 4).

4. Discussion

RNAi therapeutics have great potential for treating intractable diseases ranging from acquired diseases, such as viral infections, to purely genetic disorders. However, inefficient delivery into specific organs has hindered their clinical application.

Recently, a combination of microbubbles and US has been proposed as a less invasive and tissue-specific method of gene delivery. The combination produces transient changes in the permeability of the cell membrane and allows for the site-specific intracellular delivery of molecules such as dextran, pDNA, peptides, and siRNA both *in vitro* and *in vivo* (Du et al., 2011; Kinoshita and Hynynen, 2005; Li et al., 2003; Otani et al., 2009; Sonoda et al., 2006; Taniyama et al., 2002a,b; Tsunoda et al., 2005; Unger et al., 2004). However, because existing microbubbles have problems with size, stability, and targeting functionality, we developed liposomal bubbles (BLs). BLs are an effective and novel tool for gene and siRNA delivery *in vitro* and *in vivo* (Negishi et al., 2008, 2011b,c; Suzuki et al., 2007, 2008a,b). Our method using BLs and US did not involve endocytosis, and siRNA was directly introduced into the cytoplasm within a fairly short time. Thus, it seems unnecessary to consider the escape of siRNA from the endosome and the degradation of siRNA in lysosomes, although the endosomal escape is an important issue in other delivery tools. Furthermore transfection methods using physical energy other than US are expected and are currently being developed (Endoh and Ohtsuki, 2009; Kong et al., 2004; Oliveira et al., 2007; Schiffelers et al., 2005; Takei et al., 2008). These methods are difficult to apply to deep tissue. In contrast, US is able to control the accessible tissue sites by changing of the frequency and to reach the deep tissues. However, our previous results were obtained using a mixture of BLs and naked siRNA, which do not colocalize in blood vessels after intravenous administration. Additionally, siRNA is susceptible to degradation by nucleases and rapid removal from circulation. Consequently, these factors may cause a reduction in transfection efficiency. In this study, we prepared siRNA-loaded BLs (si-BLs) using a cationic lipid as a more effective, efficient delivery tool for systemic injections.

We initially attempted to entrap a US imaging gas in BLs containing DOTAP, a cationic lipid often used for gene delivery. Liposomes containing up to 15 mol% DOTAP did entrap the gas and could be used as ultrasound contrast agents. However, liposomes containing more than 15 mol% DOTAP had difficulty maintaining the gas. We also tested BLs containing DOTAP using a high-frequency US imaging system. An echo signal was detected as well as for BLs without DOTAP, although the imaging effect was slightly reduced 30 min later (Fig. 1). These results were assumed to be due to differences in the response to US and the stability of each BL type.

We used flow cytometry to examine the interaction between siRNA and BLs. The BLs were detectable, although the fluorescence intensity was low. The fluorescein-labeled siRNA molecules were too small to be detected with flow cytometry. However, the siRNA-loaded BLs exhibited strong fluorescence. We determined that siRNA could interact with BLs, and the interaction was due to the cationic charge of DOTAP. The amount of siRNA bound to the BLs was slightly increased in the presence of DOTAP. Furthermore, BLs containing both DOTAP and PEG_{750} could be loaded with much more siRNA (Fig. 2). BLs containing neither DOTAP nor PEG_{750} also loaded successfully with a certain amount of siRNA. These results suggested that siRNA could be loaded not only by the electrostatic interaction, but also by the fixed aqueous layer formed with PEG. It has been reported that the modification of liposomes with short and long PEG chains increases the fixed aqueous layer thickness (Sadzuka et al., 2002). We considered that the structural changes in the PEG chain facilitated interaction between the cationic lipid and anionic siRNA. Moreover, there were no significant changes in size after adding siRNA (Table 1). The data suggested that siRNA

was bound to the surface of BLs and that BLs did not aggregate. We also investigated the stability of siRNA interacting with BLs in 50% serum. Although some siRNA was degraded, siRNA held by BLs showed increased stability in 50% serum compared with free siRNA (Fig. 3). In the solution of si-BLs, free siRNA was present with si-BLs. Therefore, the siRNA not held by BLs was degraded. We examined the change in the amount of bound siRNA by adding various amounts of siRNA to BLs. As shown in Fig. 4, the amount of siRNA loaded onto BLs (60 μg) increased with siRNA addition in a dose-dependent manner up to 100 pmol.

We also investigated the effects of US exposure on si-BLs by analyzing the si-BL solution after exposure under the same conditions used for the *in vitro* transfection. No fluorescence was detected. Moreover, there were only a few detectable molecules in the solution of si-BLs after US exposure, and the histogram representing the results was almost parallel to the horizontal axis, similar to the solution of free siRNA (Fig. 5). This result suggested that US exposure collapsed si-BLs, releasing siRNA from the surface of the BLs. We confirmed that there was no damage to siRNA from US exposure by electrophoresis (data not shown). Undetectable fluorescence does not necessarily mean that siRNA were released from BLs: it is also possible that siRNA interacted with lipids or BLs that reverted to liposomes by degassing. However, the gene-silencing effects of siRNA transfection via si-BLs and US were comparable to those of siRNA transfection with conventional BLs and US (Fig. 6). Therefore, it appears that the exposure to US-induced cavitation, the release of siRNA from BLs, and the delivery of siRNA into the cytoplasm. We are currently developing BLs composed of lipids other than DPPC or DOTAP in attempts to form more stable and effective BLs. In the future, we will also examine siRNA delivery and disease-associated gene-silencing effects.

The preparation method of si-BLs developed in this study was easier than that of chol-si-BLs reported previously (Negishi et al., 2011a). Furthermore, BLs containing cationic lipid are expected to have widespread application to delivery tools of various molecules possessing negative electric charges. We confirmed that not only siRNA but also pDNA can be loaded onto BLs (p-BLs). Additionally, microbubbles conjugated to an antibody and having a targeting function have been developed recently (Behm et al., 2008; Leong-Poi et al., 2005; Palmowski et al., 2008). Liposomes can be easily modified to add a targeting function. Thus, the development of targeting si-BLs or p-BLs using an antibody or peptide is expected to lead to beneficial clinical applications for various diseases.

5. Conclusion

In this study, we showed that si-BLs could deliver siRNA as well as conventional BLs, although there remains room for improvement. Additionally, BLs containing a cationic lipid interacted with siRNA and protected the siRNA against nuclease degradation. These results suggest that si-BLs combined with US exposure may be useful for delivering siRNA to a tissue or organ via systemic injection.

Acknowledgements

We are grateful to Dr. Katsuro Tachibana (Department of Anatomy, School of Medicine, Fukuoka University) for technical advice regarding the induction of cavitation with US, to Ms. Yuko Ishii and Ms. Arisa Nakamura (School of Pharmacy, Tokyo University of Pharmacy and Life Sciences) for excellent technical assistance, and to Mr. Yasuhiko Hayakawa and Mr. Kosho Suzuki (Nepa Gege Co., Ltd.) for technical advice regarding US exposure. This study was supported by a Grant for Industrial Technology Research (04A05010) from the New Energy and Industrial Technology Development Organization (NEDO) of Japan, a Grant-in-Aid for Exploratory Research (18650146) from the Japan Society for the Promotion of Science, a Grant-in-Aid for Scientific Research (B) (20300179) from the Japan Society for the Promotion of Science, and a Grant-in-Aid for Young Scientists (B) (21790164) from the Japan Society for the Promotion of Science.

References

Allen, T.M., Hansen, C., Martin, F., Redemann, C., Yau-Young, A., 1991. Liposomes containing synthetic lipid derivatives of poly(ethylene glycol) show prolonged circulation half-lives in vivo. Biochim. Biophys. Acta 1066, 29–36.

Behm, C.Z., Kaufmann, B.A., Carr, C., Lankford, M., Sanders, J.M., Rose, C.E., Kaul, S., Lindner, J.R., 2008. Molecular imaging of endothelial vascular cell adhesion molecule-1 expression and inflammatory cell recruitment during vasculogenesis and ischemia-mediated arteriogenesis. Circulation 117, 2902–2911.

Blume, G., Cevc, G., 1990. Liposomes for the sustained drug release in vivo. Biochim. Biophys. Acta 1029, 91–97.

Delius, M., Adams, G., 1999. Shock wave permeabilization with ribosome inactivating proteins: a new approach to tumor therapy. Cancer Res. 59, 5227–5232.

Du, J., Shi, Q.S., Sun, Y., Liu, P.F., Zhu, M.J., Du, L.F., Duan, Y.R., 2011. Enhanced delivery of monomethoxypoly(ethylene glycol)-poly(lactic-co-glycolic acid)-poly l-lysine nanoparticles loading platelet-derived growth factor BB small interfering RNA by ultrasound and/or microbubbles to rat retinal pigment epithelium cells. J. Gene Med. 13, 312–323.

Duvshani-Eshet, M., Machluf, M., 2005. Therapeutic ultrasound optimization for gene delivery: a key factor achieving nuclear DNA localization. J. Control. Release 108, 513–528.

Endoh, T., Ohtsuki, T., 2009. Cellular siRNA delivery using cell-penetrating peptides modified for endosomal escape. Adv. Drug Deliv. Rev. 61, 704–709.

Frank-Kamenetsky, M., Grefhorst, A., Anderson, N.N., Racie, T.S., Bramlage, B., Akinc, A., Butler, D., Charisse, K., Dorkin, R., Fan, Y., Gamba-Vitalo, C., Hadwiger, P., Jayaraman, M., John, M., Jayaprakash, K.N., Maier, M., Nechev, L., Rajeev, K.G., Read, T., Röhl, I., Soutschek, J., Tan, P., Wong, J., Wang, G., Zimmermann, T., de Fougerolles, A., Vornlocher, H.P., Langer, R., Anderson, D.G., Manoharan, M., Koteliansky, V., Horton, J.D., Fitzgerald, K., 2008. Therapeutic RNAi targeting PCSK9 acutely lowers plasma cholesterol in rodents and LDL cholesterol in nonhuman primates. Proc. Natl. Acad. Sci. U.S.A. 105, 11915–11920.

Greenleaf, W.J., Bolander, M.E., Sarkar, G., Goldring, M.B., Greenleaf, J.F., 1998. Artificial cavitation nuclei significantly enhance acoustically induced cell transfection. Ultrasound Med. Biol. 24, 587–595.

Halder, J., Kamat, A.A., Landen, C.N., Han, L.Y., Lutgendorf, S.K., Lin, Y.G., Merritt, W.M., Jennings, N.B., Chavez-Reyes, A., Coleman, R.L., Gershenson, D.M., Schmandt, R., Cole, S.W., Lopez-Berestein, G., Sood, A.K., 2006. Focal adhesion kinase targeting using *in vivo* short interfering RNA delivery in neutral liposomes for ovarian carcinoma therapy. Clin Cancer Res. 12, 4916–4924.

Harata, M., Soda, Y., Tani, K., Ooi, J., Takizawa, T., Chen, M., Bai, Y., Izawa, K., Kobayashi, S., Tomonari, A., Nagamura, F., Takahashi, S., Uchimaru, K., Iseki, T., Tsuji, T., Takahashi, T.A., Sugita, K., Nakazawa, S., Tojo, A., Maruyama, K., Asano, S., 2004. CD19-targeting liposomes containing imatinib efficiently kill Philadelphia chromosome-positive acute lymphoblastic leukemia cells. Blood 104, 1442–1449.

Holmes, R.P., Yeaman, L.D., Taylor, R.G., McCullough, D.L., 1992. Altered neutrophil permeability following shock wave exposure *in vitro*. J. Urol. 147, 733–737.

Kim, S.H., Jeong, J.H., Lee, S.H., Kim, S.W., Park, T.G., 2008. Local and systemic delivery of VEGF siRNA using polyelectrolyte complex micelles for effective treatment of cancer. J. Control. Release 129, 107–116.

Kinoshita, M., Hynynen, K., 2005. A novel method for the intracellular delivery of siRNA using microbubble-enhanced focused ultrasound. Biochem. Biophys. Res. Commun. 335, 393–399.

Kong, X.C., Barzaghi, P., Ruegg, M.A., 2004. Inhibition of synapse assembly in mammalian muscle *in vivo* by RNA interference. EMBO Rep. 5, 183–188.

Lentacker, I., Wang, N., Vandenbroucke, R.E., Demeester, J., De Smedt, S.C., Sanders, N.N., 2009. Ultrasound exposure of lipoplex loaded microbubbles facilitates direct cytoplasmic entry of the lipoplexes. Mol. Pharm. 6, 457–467.

Leong-Poi, H., Christiansen, J., Heppner, P., Lewis, C.W., Klibanov, A.L., Kaul, S., Lindner, J.R., 2005. Assessment of endogenous and therapeutic arteriogenesis by contrast ultrasound molecular imaging of integrin expression. Circulation 111, 3248–3254.

Li, T., Tachibana, K., Kuroki, M., Kuroki, M., 2003. Gene transfer with echo-enhanced contrast agents: comparison between Albunex, Optison, and Levovist in mice—initial results. Radiology 229, 423–428.

Maruyama, K., Ishida, O., Kasaoka, S., Takizawa, T., Utoguchi, N., Shinohara, A., Chiba, M., Kobayashi, H., Eriguchi, M., Yanagie, H., 2004. Intracellular targeting of sodium mercaptoundecahydrododecaborate (BSH) to solid tumors by transferrin-PEG liposomes, for boron neutron-capture therapy (BNCT). J. Control. Release 98, 195–207.

Maruyama, K., Yuda, T., Okamoto, A., Kojima, S., Suginaka, A., Iwatsuru, M., 1992. Prolonged circulation time in vivo of large unilamellar liposomes composed of distearoyl phosphatidylcholine and cholesterol containing amphipathic poly(ethylene glycol). Biochim. Biophys. Acta 1128, 44–49.

McCaffrey, A.P., Meuse, L., Pham, T.T., Conklin, D.S., Hannon, G.J., Kay, M.A., 2002. RNA interference in adult mice. Nature 418, 38–39.

Morrissey, D.V., Lockridge, J.A., Shaw, L., Blanchard, K., Jensen, K., Breen, W., Hartsough, K., Machemer, L., Radka, S., Jadhav, V., Vaish, N., Zinnen, S., Vargeese, C.,